AD-A074 958 RENSSELAER POLYTECHNIC INST TROY N Y DEPT OF MECHANI--ETC F/G 11/6
UNIAXIAL CREEP, CYCLIC CREEP AND RELAXATION OF AISI TYPE 304 ST--ETC(U)
AUG 79 D KUJAWSKI, V KALLIANPUR, E KREMPL N00014-76-C-0231
UNCLASSIFIED RPI-CS-79-4 NL

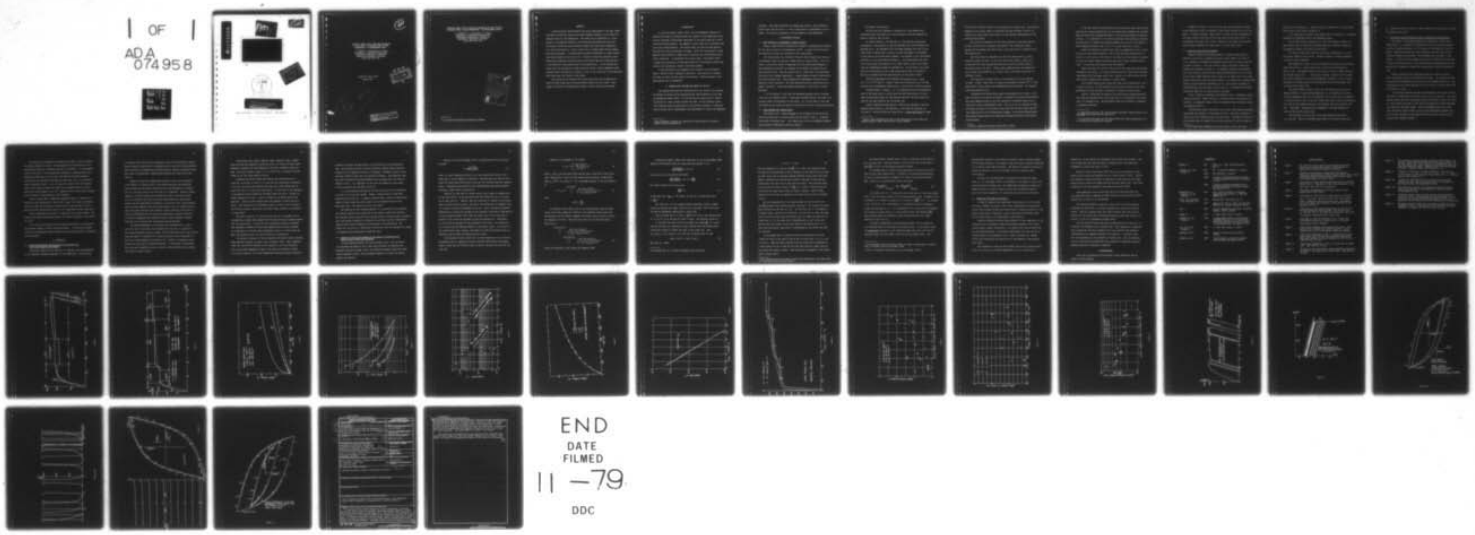

END
DATE FILMED
11-79
DDC

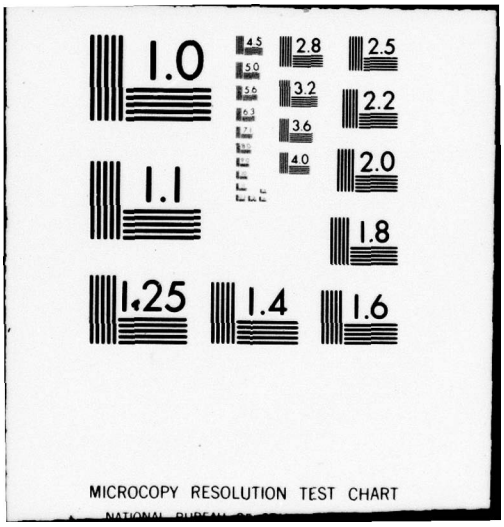
1.0
1.1
1.25
1.4
1.6
1.8
2.0
2.2
2.5
2.8
3.2
3.6
4.0
4.5
5.0
5.6
6.3
MICROCOPY RESOLUTION TEST CHART

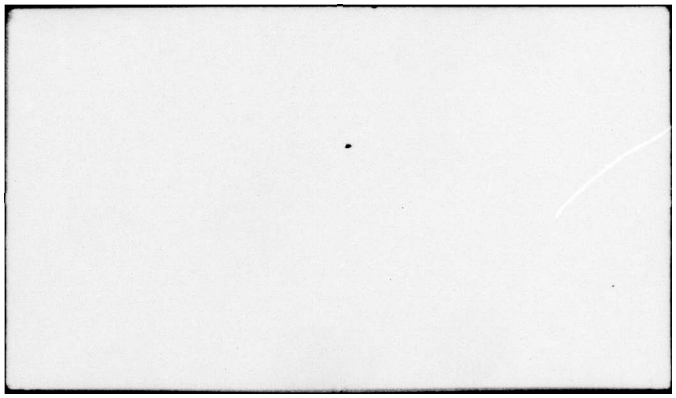

UNIAXIAL CREEP, CYCLIC CREEP AND RELAXATION OF AISI TYPE 304 STAINLESS STEEL AT ROOM TEMPERATURE. AN EXPERIMENTAL STUDY.

D. Kujawski, V. Kallianpur, E. Krempl
Department of Mechanical Engineering,
Aeronautical Engineering & Mechanics
Rensselaer Polytechnic Institute
Troy, New York 12181

Report No. RPI CS 79-4

August 1979

UNIAXIAL CREEP, CYCLIC CREEP AND RELAXATION OF AISI TYPE 304 STAINLESS STEEL AT ROOM TEMPERATURE. AN EXPERIMENTAL STUDY.

D. Kujawski[1)], V. Kallianpur, E. Krempl
Department of Mechanical Engineering,
Aeronautical Engineering & Mechanics
Rensselaer Polytechnic Institute
Troy, New York 12181

1) On leave from Technical University of Warsaw.

ABSTRACT

A servocontrolled testing machine and strain measurement at the gage length were used to study the uniaxial rate(time)-dependent behavior of AISI Type 304 Stainless Steel at room temperature. The creep strain accumulated in a given period of time depends strongly on the stress rate preceding the creep test. In constant stress rate zero-to-tension loading the creep strain accumulated in a fixed time period at a given stress level is always higher during loading than during unloading. Continued cycling causes an exhaustion of creep ratchetting which depends on the stress rate. Periods of creep and relaxation introduced during completely reversed plastic cycling show that the curved portions of the hysteretic loop exhibit most of the inelasticity. In the straight portions creep and relaxation are small and there exists a region commencing after unloading where the behavior is similar to that at the origin for virgin materials. This region does not extend to zero stress.

The results are at variance with creep theory and with viscoplasticity theories which assume that the yield surface expands with the stress. They support the theory of viscoplasticity based on total strain and overstress.

1. INTRODUCTION

In a previous paper, Krempl (1979), the rate-dependent* behavior of annealed AISI Type 304 Stainless Steel was studied at room temperature using uniaxial specimens, displacement measurement at the gage length and a servo-controlled testing machine. The emphasis in this study was on relaxation and strain-rate change behavior. The present paper utilizes the same material and identical testing techniques as Krempl (1979) but concentrates on creep behavior under monotonic loading and on relaxation and creep behavior under cyclic conditions. It complements the earlier paper. Both papers reveal a complex but consistent and repeatable behavior of this material under load (stress) and displacement (strain) controlled loading.

In the following we give examples of the behavior of this material under a variety of test (boundary) conditions. Only results are included for which at least one other check has been made. Results obtained on the same specimen are so designated.

2. MATERIAL, TEST SPECIMEN, AND METHOD OF TESTING

The annealed AISI Type 304 Stainless Steel, the uniaxial test specimen, the method of testing and the servocontrolled testing machine are the same as employed by Krempl (1979). For the plotting of creep strain or relaxation stress vs. time a second recorder was used. We use piecewise linear test histories (only the ramp option of the function generator is used) and control either load or displacement with displacement or load as the dependent

---

* Rate-dependence includes rate sensitivity under monotonic and cyclic loading, creep and relaxation.

variables. From these quantities the engineering stress σ (load divided by initial area) and the strain $\epsilon = \Delta\ell/\ell$ (ℓ gage length of extensometer) are obtained. All tests are performed in air environment at room temperature.

3. EXPERIMENTAL RESULTS

3.1 Load (Stress) vs. Displacement (Strain) Control

Figure 1 shows that the stress-strain response is fundamentally different for the case of load and of displacement control In each case the specimen was loaded by the same time variations of the input-signal.

For stress control the transition from the initial quasilinear region to the nonlinear region is much more gradual than for strain control. For a decrease in rate by two orders of magnitude the flow stress drops abruptly in the displacement controlled case whereas little change is observed for the load controlled case. When the loading rate is raised again the displacement controlled curve responds immediately. A small change in slope is observed for the load controlled case. Upon unloading the displacement controlled curve exhibits a sharp transition. The load controlled curve is characterized by a gradual transition. Both curves become equidistant to each other as stress decreases.

It is of interest to note that the unloading branches are not straight lines, but are slightly curved. In the upper unloading portion the slope is at one point equal to the modulus at the origin. At $\sigma = 0$ the slope is less than the modulus at the origin for both the stress and the strain controlled condition.

3.2 Creep Behavior for Step-up Tests

The stress-total strain diagrams of two specimens (No.II and No.III) which were subjected to a step-up creep test are given in Fig.2. In between the periods of constant load the loading rate of the two specimens differed by two orders of magnitude as shown in Figure 2.

We observe the following:

At each load level specimen II subjected to a high loading rate accumulates more creep strain in a given period of time than specimen III which is loaded at the low rate.

At stress levels σ_2 = 220 MPa and σ_3 = 232.6 MPa the creep strain accumulated in five minutes is equal for specimen No.III but different for specimen No.II. For specimen No.III the slope preceding the start of the creep tests at stress level σ_2 and σ_3 is equal and appears to correspond to the slope of the stress strain diagram. For specimen II the slope before reaching σ_2 is less than before reaching σ_3. The slopes before the start of the creep tests with specimen II at stress levels σ_2 and σ_3 are higher than the corresponding slopes for specimen III. At the start of the creep tests at stress-levels σ_2 and σ_3 the stress-strain curve of specimen II has not yet reached the slope characteristic of the plastic range*.

The above experiments were repeated with specimen No.IV, tested at $\dot{\sigma} = 6.9 \times 10^{-2}$ MPa s^{-1}. Figure 3 shows the creep curves at σ_1 = 187 MPa and Fig.4 the corresponding creep rates vs. total strain for three specimens.

Although there is scatter, i.e., the different curves for specimens III and IV, the creep rate at a given strain and the creep strain at a given time are definitely higher for the specimen tested at the high stress rate than for the ones tested at the low stress rate.

Figure 5 shows the creep rates vs. total strain measured at the subsequent stress levels σ_2 = 220 MPa and σ_3 = 232.6 MPa for specimens II, III and IV. We see now that the creep rate at a <u>given total strain</u> is equal

---

* Plastic range designates the part of the stress-strain curve where the tangent modulus is much less than the initial modulus.

for specimens II and III tested at the high and the low stress rate. This behavior, measured in the plastic range, is different from the one shown in Fig.4, obtained at the first stress level which is at the sharply curved portion of the stress-strain diagram.

The curves for specimens III and IV are parallel to each other and can be made coincident by a horizontal translation*. Due to material scatter specimen IV has reached the stress level of the creep test at a smaller strain than specimen III.

The creep curves for specimens III and IV at stress levels σ_2 and σ_3 coincide as shown in Fig.6. We note that the stress levels σ_2 and σ_3 are 220 MPa and 232.6 MPa, respectively and that the initial strains differ at each stress level, see Fig.5. Despite these differences and the differences in the creep curves shown for σ_1 in Figs.3 and 4, one single creep curve is obtained in Fig.6.

The creep test at stress level σ_3 with specimen IV was continued for 24 hours. Figure 7 shows that the creep rate decreased to nearly 10^{-8} s^{-1} and that nearly 1% creep strain was accumulated during this period. No secondary creep was obtained at all.

Considering the stress-strain graph for specimen No.III in Fig.2 we see that the periods of creep do not appear to influence the stress-strain behavior. The final dashed portions of the curve obtained at increasing stress can be connected to form a stress-strain curve. This is not so for specimen II where the slopes just prior to the start of the creep test are much higher than the ones characteristic of the stress-strain diagram. A continued loading beyond the required creep stress level would have decreased the slope of the stress-strain diagram.

---

* This fact explains the single creep curve in Fig.6.

In the next series of tests loading was continued and creep tests started only when the slopes characteristic of the stress-strain diagrams were reached*. Typical stress-strain diagrams obtained in this testing procedure are depicted in Fig.8. It is important to note that the portions with increasing stress can be connected to a stress-strain diagram (dashed lines) and that the slopes of these diagrams are almost equal for the two stress rates used in Fig.8.

Results of additional step-up creep tests are summarized in Fig.9, where we plot the creep strain obtained in 300 s (the horizontal distances a-b in Fig.8) vs. total strain at the start of the creep test (total strain at points a in Fig.8) for seven different specimens subjected to three different stress rates. In each case only primary creep was observed.

Again the stress rate prior to the start of the creep test significantly influences creep strain. At a given initial strain the creep strain increases considerably with increasing stress rate. Further at a given stress rate the creep strain increases with increase in initial strain.

The relation between creep stress and creep strain accumulated in 300 s is shown in Fig.10. We see that both the stress level and the stress rate preceding the creep test have a significant influence on creep strain.

Figure 11 shows that the slope of the stress-strain diagram preceding† the creep test decreases with total strain but is not affected by the stress rate in a systematic way. The differences shown are attributed to specimen-to-specimen variations.

---

* It should be noted that this test procedure precludes a specification of an arbitrary stress level of the creep test.

† We note that the creep test was started after the slope characteristic of the stress-strain diagram was obtained.

Comparison of Figs.6, 9 and 10 reveals that the coincidence of creep curves exhibited in Fig.6 is possible if the initial strains are not too far apart. In general, however, creep strain in a given time period depends on the total strain at the start of the creep test and the creep stress*. It also appears from Figs.9 and 11 that a decrease of the slope of the stress-strain diagram increases the creep strain in a given time period.

3.3 Creep for Zero-to-Tension Loading

Repeated loading and unloading behavior including creep periods is depicted in Fig.12 for a specimen with prior cyclic loading (25 cycles at ± .4%, specimen was unloaded from maximum tensile strain to zero stress and reloaded in tension). First, two cycles of stress controlled loading are imposed which terminate at point B. On subsequent loadings and unloadings the stress was held constant during loading and unloading for 120 s at each of the stress levels indicated by the arrows on the right side of the figure. Before starting the cycle with creep periods at C, a loading and unloading cycle without creep periods was introduced, see CD. Also partial unloading was performed before the last cycle, see FG in Fig.12. The maximum and minimum stress were equal for all cycles (point G excluded).

First we observe a decrease of the ratchet strain at subsequent cycles, compare OA with AB. Compare further BC, CE and GH where creep periods were inserted. A negligible ratchet strain is produced by the continuous loading and unloading cycle CD.

Following the loading from point B we see that creep develops gradually and depends very strongly on the stress level as a very small increase can cause a more than twofold increase in creep strain. The amount of creep at a given stress level is highest for the cycle starting at B and the least for

---

* Prior loading rate influences the initial strain of the creep test.

the last cycle starting at G. Indeed no creep is observed at the three lowest stress levels in the cycle starting at G.

It is interesting to observe that neither the full unloading DC nor partial unloading FG eliminated creep on the subsequent cycles.

For the three cycles, starting at B, C and E the amount of creep at a given stress level is less during unloading that during loading, compare the corresponding distances ab with cd at each cycle.

The results clearly show that the creep strain accumulated in a given time cannot depend on stress alone. Further we observe a gradual exhaustion of creep as strain increases.

The exhaustion of creep is also confirmed by the results of Fig.13 where after some cycles at a given stress rate $\dot{\sigma}_1$ the rate was decreased by a factor of ten. The maximum stress of this series of tests is about 10% below the maximum stress level during prior history. Despite this low stress level creep ratchetting occurs and considerable influence of rate is evident. The amount of ratchet strain per cycle decreases with each subsequent cycle at each constant stress rate.

The results shown in Figs.12 and 13 are for specimens with prior mechanical history. The qualitative behaviors, i.e. the exhaustion of creep with each subsequent cycle and the difference in the creep strain accumulated in a given period of time at the same stress level during loading and unloading was found for the annealed condition and specimens with prior monotonic and cyclic preloading. The quantitative dependence is strongly dependent on prior history and the stress level.

The influence of stress level can be appreciated by noting that no creep was found at a maximum stress equal to the lowest stress level

σ_o = 180 MPa in cycle BC in Fig.12. This stress level is only about 14% below the maximum stress level.

3.4 Periods of Creep and Relaxation during Completely Reversed Cycling

The results to be presented shortly were obtained in a quasi cyclic steady state, i.e., annealed or specimens with prior history were subjected to strain controlled cycling at ± 0.4% strain till the hysteresis loop was stable. Relaxation periods were then introduced around the loop and the relaxation behavior was observed. Other specimens were switched to load control. In these cases the maximum stress level was below the one obtained in strain controlled cycling. After some additional adjustment cycles creep periods were introduced to observe the creep behavior around the hysteresis loop.

Figure 14a depicts such experiments which were started at point a, below the maximum stress of the completed 12th cycle. All consecutive creep hold periods are designated by the letters of the alphabet ending at w. The corresponding creep curves observed in 300 s are given in Fig.14b which plots total strain vs. time.

In the nearly straight sections of the hysteresis loop creep is either very small or nonexistent, see curves b,c,d,e; n,o,p,w in Fig.14b. Very little reverse creep (creep rate has opposite sign of the stress) is seen at f and p. At g and q which are points of zero stress the magnitude of strain decreases by a small but noticeable amount. Below the maximum stress level of the cycle additional creep is found (a,v,m,n) which subsequently subsides (b,c, d,o) and then increases in the opposite direction as the curvature of the stress-strain diagram increases.

The results for intermittent relaxation tests shown in Fig.15 confirm the results obtained in creep. At the completion of the 204th cycle 300 s relaxation periods were introduced starting at a through u. At the maximum strain of the cycle a and ℓ, significant relaxation is observed which subsequently resides (b,c,d; m,n,o) and is followed by reversed relaxation (total strain and relaxation rate have the same sign, f-i; o-t) followed by normal relaxation (j,k;u). It is of interest to observe that the absolute value of the stress increases by a small but noticeable amount at p and f. Further the stress change in the 300 s relaxation test is observed to increase as the curvature of the hysteretic loop increases.

Figure 16 shows that a completely analogous behavior is obtained for relaxation tests performed on a loop within a loop. This time no relaxation curves are shown but the places at which the 300 s hold periods are introduced are either identified by arrows or are recognizable by the stress drop.

Also we performed creep tests in a hysteresis loop within another. The results were qualitatively those found in 14a and are analogous to the relaxation case.

As in the zero-to-tension case the qualitative behavior was reproduced for specimens having a variety of prior histories. In the nearly straight sections of the hysteresis loop inelasticity is practically absent irrespective of prior history.

4. DISCUSSION

4.1 General Observations and Implication of the Results for Constitutive Equation Development

The results shown in Fig.1 may serve to illustrate why rate-dependence is not generally considered important at room temperature. First one has

to recognize that strain control represents a very stiff conventional testing machine whereas stress control is representative of very soft testing machines. The screw-driven or hydraulically operated machines without servocontrol which were used in the past have a characteristic between the stiff and the soft variety.

Suppose now that rate changes such as shown in Fig.1 are simulated on a soft machine, a response close to the stress-controlled case would have been obtained with the obvious conclusion that rate dependence is insignificant in a situation where we now know that it is important. Further, without changes in rate the stress-strain diagrams for stress- and strain-control are not so different that they would have caused reason for concern when results from the same material obtained on a stiff and a soft testing machine would have been compared (see the initial portion of the σ-ε diagram in Fig.1 where the strain-controlled case exhibits a sharp transition from elastic to inelastic deformation and the stress-controlled shows a gradual transition. It should be remembered that stress and strain control represent extremes which may not be realized with conventional testing machines).

The observed dependence of the creep strain accumulated in a given period of time on the stress rate preceding the creep test is analogous to the relaxation behavior found by Krempl (1979) who has shown that in the plastic range the amount of relaxation in a given time period was only dependent on the strain rate preceding the relaxation test. However, a difference exists between the creep and the relaxation behavior. In the present investigation the creep strain depends not only on the prior stress rate but also increases with strain as shown in Fig.9.

Creep theory, Hult (1966), Odquvist (1966), Rabotnov (1969), assumes that the creep rate depends on stress and time or on stress and creep strain depending on whether the time hardening or the strain hardening theory are used. The results shown in Figs.3, 4, 5, 9 and 10 are at variance with this theory as are the results shown in Fig.12.

Comparing the results during the loading and unloading portion of cycles BC, CE and GH, in Fig.12 it is seen that the creep strain accumulated in a given time period and therefore the creep rate cannot depend only on stress and time or on stress and creep strain. If this were so the difference in the behavior during loading and unloading should not exist. Further the gradual exhaustion of creep as shown in cycles BC, CE and EH could not be explained. Rather the data suggest that creep depends on stress and total strain. This implication is confirmed by Figs.2, 4 and 5 as well as Figs.9 and 10 which, however, extend into the plastic range normally not considered in creep theory.

The data in Figs.12, 13, 14a and 16 are also not in agreement with a viscoplasticity theory which assumes that the elastic-plastic boundary expands with the stress point. If this were so no inelasticity should be observed when subsequent stresses are within the expanded elastic-plastic boundary. It is important to note that creep ratchetting occurs at a stress below and above the prestress level, see Fig.13 and Fig.12, respectively.

The results of Figs.14 - 16 can be compared with similar results obtained under monotonic loading, see Figs.3 and 5 of Krempl (1979). This comparison shows that the behavior obtained in the unloading legs of the hysteresis loop is very much comparable to that at the origin for monotonic loading. It is seen in Figs.12, 14 - 16 that immediately following unloading creep, and

relaxation rate have the same sign as in the loading leg of the hysteretic loop. As unloading continues creep and relaxation subside before creep and relaxation in the opposite direction is developed. Therefore a point of zero creep and relaxation must exist by continuity arguments. Upon departure from this point inelasticity develops gradually and is present when the stress is reduced to zero. It is important to note that this behavior is also found in the loop within the loop shown in Fig.16.

It is also apparent from Figs.14 - 16 that this point of zero relaxation or stress is not very well defined. Rather a region exists in which this preferred point could lie. It appears therefore that a region of inelasticity similar to that around the origin exists in the unloading portion of the hysteresis loop. This region is not at zero stress.

The modeling of this unloading behavior is a challenge for any constitutive theory, especially for those that do not employ a yield-like condition. The materials science oriented state variable theories in which the state variables grow continuously according to a system of first-order nonlinear differential equations will find the modeling of this behavior very challenging. The authors are not aware of a theoretical investigation that has addressed the change in relaxation and creep behavior around the loop.

4.2 Relation of the Present Results to the Theory of Viscoplasticity Based on Total Strain and Overstress

We have shown previously, see Liu and Krempl (1979), that the theory of viscoplasticity based on total strain and overstress can reproduce the phenomena reported by Krempl (1979), the difference between stress and strain control depicted in Fig.1, and the gradual exhaustion of creep for tension-tension load cycling.

When Eq.(1) of Liu and Krempl (1979) is specialized for the creep test we obtain

$$\dot{\epsilon} = \frac{\sigma_o - g[\epsilon]}{Ek[\sigma_o - g[\epsilon]]} \qquad (1)$$

where ϵ is total engineering strain, σ_o is the constant true stress of the creep test, E is the modulus of elasticity. The functions $g[\epsilon]$ and $k[\sigma - g[\epsilon]]$ denote the equilibrium stress-strain curve and the viscosity function, respectively. A superposed dot stands for time differentiation and square brackets following a symbol denote "function of".

Equation (1) says that at a given stress σ_o the creep rate depends only on the total strain. We see from Fig.4 that the results for $\sigma_1 = \sigma_o = 187$ MPa do not agree with (1). However, when the creep test is started in the plastic range at stress levels σ_2 and σ_3 (see Fig.2) the results are in agreement with (1) as shown in Fig.5 for specimens II and III. (Due to specimen-to-specimen differences the results for specimen IV are different from those of specimen III. It can be seen from Figs.4 and 5 that the stress level of the creep test is reached at less strain for specimen IV than for specimen III. Accordingly all the curves for specimen IV are translated to the left.) The predictions of (1) agree with the observed behavior in the plastic range. At the knee of the stress-strain curve, however, the behavior of AISI 304 Stainless Steel is different from the behavior predicted by the theory.

The influence of prior stress rate on creep deformation can of course be accounted for by (1) through the initial condition which enters nonlinearly. Figure 2 shows that the initial strain is less for the fast test than for the slow test.

Separation of variables in (1) yields

$$t - t_o = E \int_{\epsilon_o}^{\epsilon} \frac{k[\sigma_o - g[\epsilon^*]]}{\sigma_o - g[\epsilon^*]} d\epsilon^* \qquad (2)$$

where ϵ_o and t_o are the total strain and the time at the start of the creep test, respectively, t and ϵ are the current time and strain, respectively. Using $\sigma_o - g[\epsilon^*] - (\sigma_o - g[\epsilon_o]) = \gamma$ as a new dummy variable (2) can be rewritten as

$$t - t_o = -E \int_{o}^{g[\epsilon_o]-g[\epsilon]} \frac{k[\gamma + (\sigma_o - g[\epsilon_o])]}{(\gamma + (\sigma_o - g[\epsilon_o]))g'[\epsilon^*]} d\gamma \qquad (3)$$

where

$$g'[\epsilon^*] = \frac{dg}{d\epsilon^*} .$$

We consider now two creep tests on the same specimen, using the same stress rate during loading but started at two different stress levels and corresponding initial strains (example, the stress levels σ_2 and σ_3 in Fig.2 for specimen II or III). The creep tests last for the same time period. Then from (3)

$$\int_{o}^{(g[\epsilon_o]-g[\epsilon])_1} \frac{k[\gamma + (\sigma_o - g[\epsilon_o])_1]}{(\gamma + (\sigma_o - g[\epsilon_o])_1)g'[\epsilon^*]} d\gamma =$$

$$\int_{o}^{(g[\epsilon_o]-g[\epsilon])_2} \frac{k[\gamma + (\sigma_o - g[\epsilon_o])_2]}{(\gamma + (\sigma_o - g[\epsilon_o])_2)g'[\epsilon^*]} d\gamma \qquad (4)$$

where the subscripts 1 and 2 denote two separate tests.

Cernocky and Krempl (1979a) have shown that (1) of Liu and Krempl (1979) exhibits the following limits for large time and constant $\dot{\epsilon}$ or $\dot{\sigma}$,

$$\frac{\{\sigma - g[\epsilon]\}}{k[\{\sigma - g[\epsilon]\}]} = (E - g')\dot{\epsilon} \tag{5}$$

for strain control and and for both cases

$$\frac{\{\sigma - g[\epsilon]\}}{k[\{\sigma - g[\epsilon]\}]} = (E - g')\,\dot{\sigma}\left\{\frac{d\epsilon}{d\sigma}\right\} \tag{6}$$

for stress control and for both cases

$$\left\{\frac{d\sigma}{d\epsilon}\right\} = g' \tag{7}$$

In the above $\{A\} \equiv \lim_{t\to\infty} A$. The limits (5) and (6) are equivalent since $\dot{\sigma} = \frac{d\sigma}{d\epsilon}\,\dot{\epsilon}$.

The limits (5) - (7) are rapidly attained asymptotic limits as demonstrated by Cernocky and Krempl (1979) and Liu and Krempl (1979) and we may use them as approximate expressions at finite time.

Next we assume that $g' = \text{const.} = \frac{d\sigma}{d\epsilon} \neq 0$ for finite time and then from (7) or (6) or (5) we see that $\{\sigma - g[\epsilon]\} = \text{const.}$ The solution "locks in".

To interpret the tests of Fig.2 we assume that indeed $\frac{d\sigma}{d\epsilon} = g' = \text{const.}$* and that the tests are conducted in such a way that the real stress-strain curves have "locked in" before the start of the creep test. Then $(\sigma_o - g[\epsilon_o])_1 = (\sigma_o - g[\epsilon_o])_2 = \{\sigma - g[\epsilon]\}$ and it follows from (4) that

$$(g[\epsilon_o] - g[\epsilon])_1 = (g[\epsilon_o] - g[\epsilon])_2 \tag{8}$$

and since $g' = \text{const}$

---

* We presume that g' is constant throughout the creep tests.

$$(\epsilon - \epsilon_o)_1 = (\epsilon - \epsilon_o)_2 . \qquad (9)$$

With the assumption of "lock-in" and $\frac{d\sigma}{d\epsilon} = g' = \text{const.}$ the overstress model can predict the observations of Fig.2, Specimen III and Fig.6 which show that the same creep curve is obtained although different stress levels were used. Figure 2 (Specimen III) and the test records of specimen IV show that the slopes before the start of the creep tests are equal. The overstress model also says that if either "lock-in" or $\frac{d\sigma}{d\epsilon} = g' = \text{const.}$ or both are not fulfilled then the creep curves cannot be equal in general. Both of these conditions are not true for specimen II at stress level σ_2 and σ_3 and shown in Fig.2.

For the interpretation of the results shown in Fig.9 we first note that $\frac{d\sigma}{d\epsilon}$ decreases with increasing strain, see Fig.11. We consider two creep tests starting with the same $\sigma_o - g[\epsilon]$. For the first test g' is assumed to be always larger than for the second test. We note from (1) that the creep rate for the first test after the initial point is always less than for the second test [in (1) the creep rate is determined by $\sigma_o - g[\epsilon]$ alone; this quantity decreases faster for the first than for the second test.]* In a given time period more creep strain is accumulated for the second test than for the first.

We now assume that (7) holds and that the stress-strain curve has "locked-in" prior to the start of any of the two creep tests, i.e., $\sigma_o - g[\epsilon] = \{\sigma - g[\epsilon]\}$. Then our theory predicts that the creep strain accumulated in a given period of time is less for the first test ($d\sigma/d\epsilon$ is large) than for the second test ($d\sigma/d\epsilon$ is small). This prediction corresponds to the results shown in Figs.9 and 11.

---

* This reasoning can also be used to explain the difference in the creep rates vs. total strain shown in Figs.4 and 5.

The above however, assumes that $\{\sigma - g[\varepsilon]\}$ is identical at the start of the two creep tests. This may, however, not be true for the case of Fig.11 where $\frac{d\sigma}{d\varepsilon} \ll E$ and a slowly varying function of strain.

If we assume that (7) holds for this condition we see from (5) and (6) that $\{\sigma - g[\varepsilon]\}$ must change with g'. Moreover in the stress-controlled case $\{\sigma - g[\varepsilon]\}$ is more sensitive to changes in g' than in the strain-controlled case. From (5), (6) and the chain rule we can obtain

$$\left.\frac{\partial\{\sigma - g[\varepsilon]\}}{\partial g'}\right|_{\dot{\sigma}=\text{const}} = \frac{E}{g'} \left.\frac{\partial\{\sigma - g[\varepsilon]\}}{\partial g'}\right|_{\dot{\varepsilon}=\text{const}} . \quad (10)$$

*

If we admit that (5) - (7) apply for finite time then $\{\sigma - g[\varepsilon]\}$ must change with g' with the greatest effect in the stress-controlled case. According to (6) a decrease in g' causes an increase in $\{\sigma - g[\varepsilon]\}$ if $k' = \frac{dk[x]}{dx} < 0$ +. An increase in the initial $\{\sigma - g[\varepsilon]\}$ corresponds to an increased initial and subsequent creep rate according to (1). So if adjustments of $\{\sigma - g[\varepsilon]\}$ occur they enhance the increase of creep strain in a given period of time with decreasing $\frac{d\sigma}{d\varepsilon}$. The overstress model can therefore account qualitatively for the trends observed in Figs.9 and 11.

The above interpretation gives additional support to the validity of the overstress model for AISI Type 304 Stainless Steel. In the plastic range the qualitative properties of the overstress model agree very well with experimental data, see also Krempl (1979) and Liu and Krempl (1979). The

---

* A bias between stress and strain control is found in experiments, see Fig.1 and in our model, see Liu and Krempl (1979)

+ This is a desirable restriction, see Liu and Krempl (1979).

discrepancies reported in Fig.4 before the plastic range is reached suggest that the model may need to be changed so that the present properties exhibited in the plastic range remain unaltered. The addition of second derivatives of stress and strain to (1) of Liu and Krempl (1979) is presently under investigation.

Presently the overstress model as proposed by Cernocky and Krempl (1979 a), Liu and Krempl (1979), is considered a valid model as long as the overstress does not change sign. The augmentation proposed by Cernocky and Krempl (1979b,c) for cyclic loading are such that the behavior shown in Figs.14-16 can be reproduced in a qualitative way without any difficulty.

4.3 Comparison with Other Test Results

A recently completed room temperature investigation of a Ti-7-Al-2Cb-1Ta alloy, Kujawski and Krempl (1979), shows considerable rate sensitivity of this high strength,low-ductility material and a relaxation behavior in the plastic range which is analogous to that of AISI Type 304 Stainless Steel. The overstress model is also applicable to this material.

Relaxation behavior and rate change behavior at room temperature in the curved portions of hysteresis loops were studied by Burbach (1970) using a testing machine without servocontrol. His results agree qualitatively with the ones reported herein. No relaxation measurements are given for the unloading portion of the hysteretic loop. Elastic unloading was assumed. Inverse rate sensitivity was observed for an age-hardening, high-strength Al-Cu alloy.

The dependence of creep on prior loading rate was also found by Tilly (1972) for tests run at elevated temperature on an 11 Cr steel and on

Nimonic 90. As the loading rate increases initial creep rate increases. The very limited data show that the effect of loading rate on the creep curve disappears at large creep times (> 10 hr).

Darlaston, Miller and Stanley (1975) also report on the effect of prior loading rate on creep and relaxation for a 1% Cr-Mo-V steel at 550°C. A permanent influence on the creep curves is reported and creep rates for the slower loading rate are found to be higher than for the fast loading rate. This trend is opposite to the one reported in this study and by Tilly (1972).

Room temperature creep of AISI Type 304 and 316 Stainless Steel has been reported by Ellis, Robinson and Pugh (1978,1979) but the effect of prior loading rate on creep is not investigated.

The relaxation behavior reported in Figs.15 and 16 was also found by Swindeman and Pugh (1979) at elevated temperature for austenitic stainless steels. They also reported creep test results showing that creep rate was different at the same stress level during step-up and step-down loading, see Figs.30, 31 and 33 of Swindemann and Pugh (1978).

The data reported herein show that the same stress level creep rate is different for different initial loading rates. This observation is important when conventional test data (loading rate is not reported) from different investigations are compared and found to be different. A possible source for the discrepancies is the influence of loading rate. This is especially true for creep tests performed after prior mechanical loading when only the maximum prestress or prestrain is reported.

ACKNOWLEDGEMENT

This work was supported by the National Science Foundation and the Office of Naval Research.

REFERENCES

Burbach, J.	1970	Techn. Mit. Krupp Forsch.-Berichte, 28, 55.
Cernocky, E.P. and Krempl, E.	1979	Int. J. Nonlinear Mechanics, in press.
	1979a	Acta Mechanica, in press.
	1979b	A Theory of Thermoviscoplasticity Based on Infinitesimal Total Strain, RPI Report CS 79-1.
	1979c	A Theory of Thermoviscoplasticity for Uniaxial Mechanical and Thermal Loading, RPI Report CS 79-3.
Darlaston, B.J., Miller, K.J. and Stanley, P.	1975	Proc. Creep and Fatigue in Elevated Temperature Applications, I. MECH ENG, LONDON, 232.1.
Ellis, J.R., Robinson, D.N. and Pugh, C.E.	1978	Nuclear Eng. and Design, 47, 115.
	1979	Paper L12/3, 5th Int. Conf. on Structural Mechanics in Reactor Technology, Berlin.
Hult, J.	1966	Creep in Engineering Structures, Blaisdell, Waltham, Toronto, London.
Krempl, E.	1979	J. Mech. Phys. Solids, in press.
Kujawski, D. and Krempl, E.	1979	An Experimental Study of the Rate(Time)-Dependent Behavior of a Ti-7AL-2Cb-1Ta Alloy under Monotonic and Cyclic Loading at Room Temperature, RPI Report CS 79-5
Liu, M.C.M. and Krempl, E.	1979	J. Mech. Phys. Solids, in press.
Odquvist, F.K.G.	1966	Theory of Creep and Creep Rupture, Oxford.
Rabotnov, Yu.N.	1969	Creep Problems in Structural Members, North Holland, Amsterdam, London.

FIGURE CAPTIONS

Figure 1 — The Influence of Load (Stress) and Displacement (Strain) Control on the Stress-Strain Behavior under Changes in Loading Rate Involving Two Orders in Magnitude

Figure 2 — Influence of Stress Rate on Subsequent Creep Behavior. Creep tests are performed at three different stress levels (arabic subscripts denote the stress level) using constant stress rate loading between the stress levels.

Figure 3 — Creep Curves of Three Different Specimens Tested at the Same Stress Level σ_1. Specimens III and IV were subjected to the same stress rate prior to the creep test.

Figure 4 — Creep Rates Corresponding to the Creep Curves of Fig.3 Plotted Versus Total Strain

Figure 5 — Creep Rates vs. Total Strain at Stress Levels $\sigma_2 = 220$ MPa and $\sigma_3 = 232.6$ MPa. The stress levels are in the plastic range. Subscripts denote the stress level. The loading rate is 6.9 MPa s^{-1} for specimen II and 0.069 MPa s^{-1} for specimens III and IV.

Figure 6 — Creep Curves for Two Different Specimens (III and IV) with the Same Stress Rate During Loading. The stress levels $\sigma_2 = 220$ MPa and $\sigma_3 = 232.6$ MPa are used and one creep curve is obtained. Subscripts denote stress level.

Figure 7 — Creep Rate vs. Time for Specimen IV for a 24 Hour Test. (Continuation of test IV_3 in Fig.6 with $\sigma_3 = 232.6$ MPa) Only primary creep is obtained.

Figure 8 — Stress-Strain Diagrams During Step-up Creep Tests. Creep tests of 300 s duration are started only after a slope characteristic of the stress-strain diagram is obtained.

Figure 9 — Creep Strain Accumulated in 300 s vs. Total Strain at the Start of the Creep Test for Three Different Stress Rates. Each symbol denotes a different specimen and the test procedure of Fig.8 is used.

Figure 10 — Creep Strain Accumulated in 300 s vs. Stress Level of Creep Test. Same tests as in Fig.9.

Figure 11 — The Slope of the Stress-Strain Diagram Immediately Preceding the Start of the Creep Test vs. Total Strain. Same tests as in Fig.9

Figure 12 Zero-to-Tension Stress-Controlled Loading with and without creep periods. Cycles OAB, CDC and EFG are without creep periods. In all other cycles 120 s creep periods are introduced at the stress levels designated by arrows. Maximum stress is 5% above maximum prestress. Prestrain refers to the strain at $\sigma = 0$.

Figure 13 Influence of Stress Rate on Creep Ratchetting. Note that σ_{max} in this figure is about 10% below the maximum prestress. Prestrain refers to the strain at $\sigma = 0$.

Figure 14a Intermittent Creep Periods of 300 s Duration During Cycling between $\pm$ 221 MPa. The creep periods start at a and end at w. The creep periods widen the hysteresis loop.

Figure 14b Total Strain vs. Time for the Creep Tests Depicted in Fig.14a Showing the Difference in Creep Behavior at Various Portions of the Hysteretic Loop

Figure 15 Relaxation Periods of 300 s Duration During Strain-Controlled Cycling at $\pm$ 0.4%. The hysteresis loop and the stress vs. time curves for one branch of the hysteresis loop are shown. The hysteresis loop is shifted due to the introduction of hold periods.

Figure 16 Relaxation Periods During Cyclic Steady-State Loading Using the Procedure of Fig.15. (The stress vs. time curves are not shown.) Relaxation is observed for the loop within the loop.

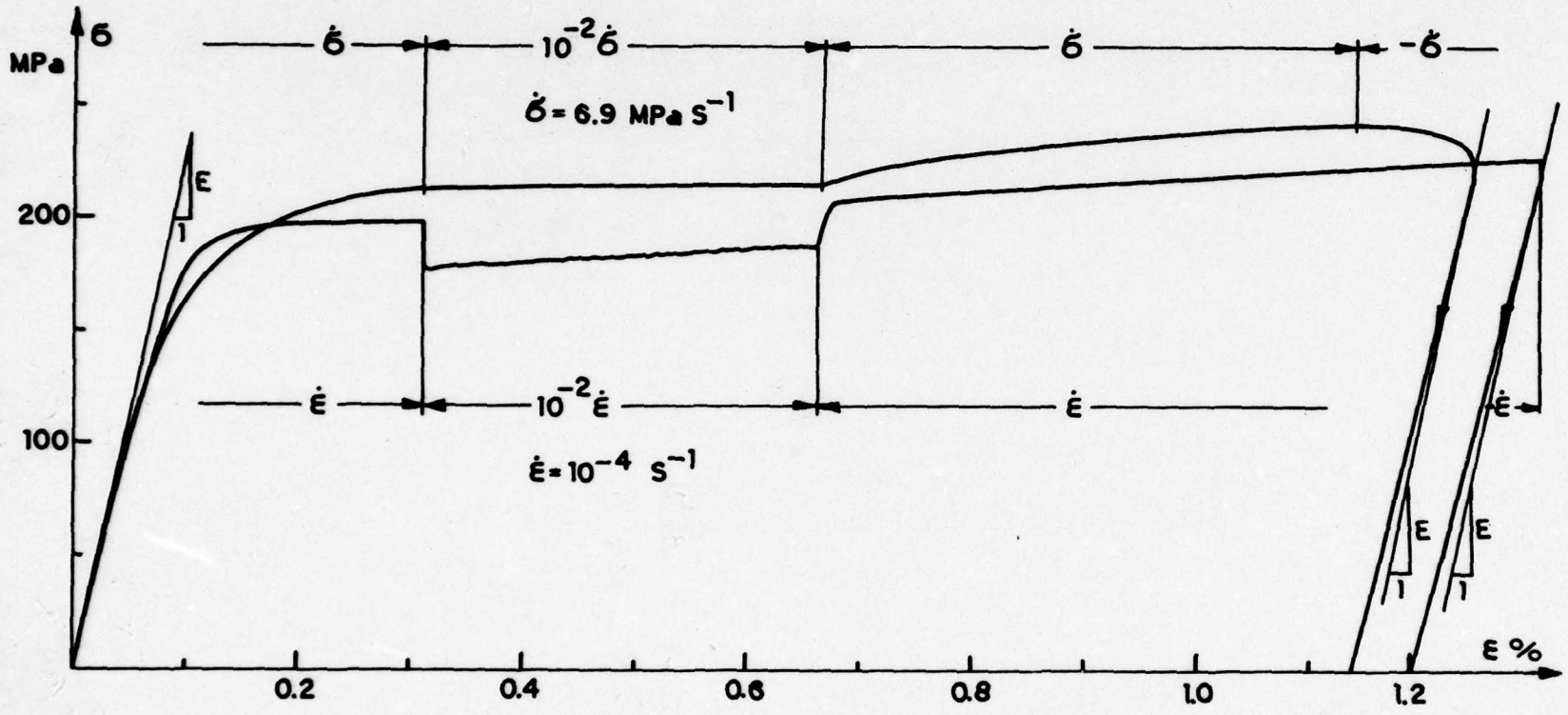
σ
MPa
σ̇
10⁻²σ̇
σ̇
-σ̇
σ̇ = 6.9 MPa s⁻¹
E
1
200
100
ε̇
10⁻²ε̇
ε̇
ε̇ = 10⁻⁴ s⁻¹
E
1
E
1
ε̇
E
1
E
1
ε %
0.2
0.4
0.6
0.8
1.0
1.2

Figure 1

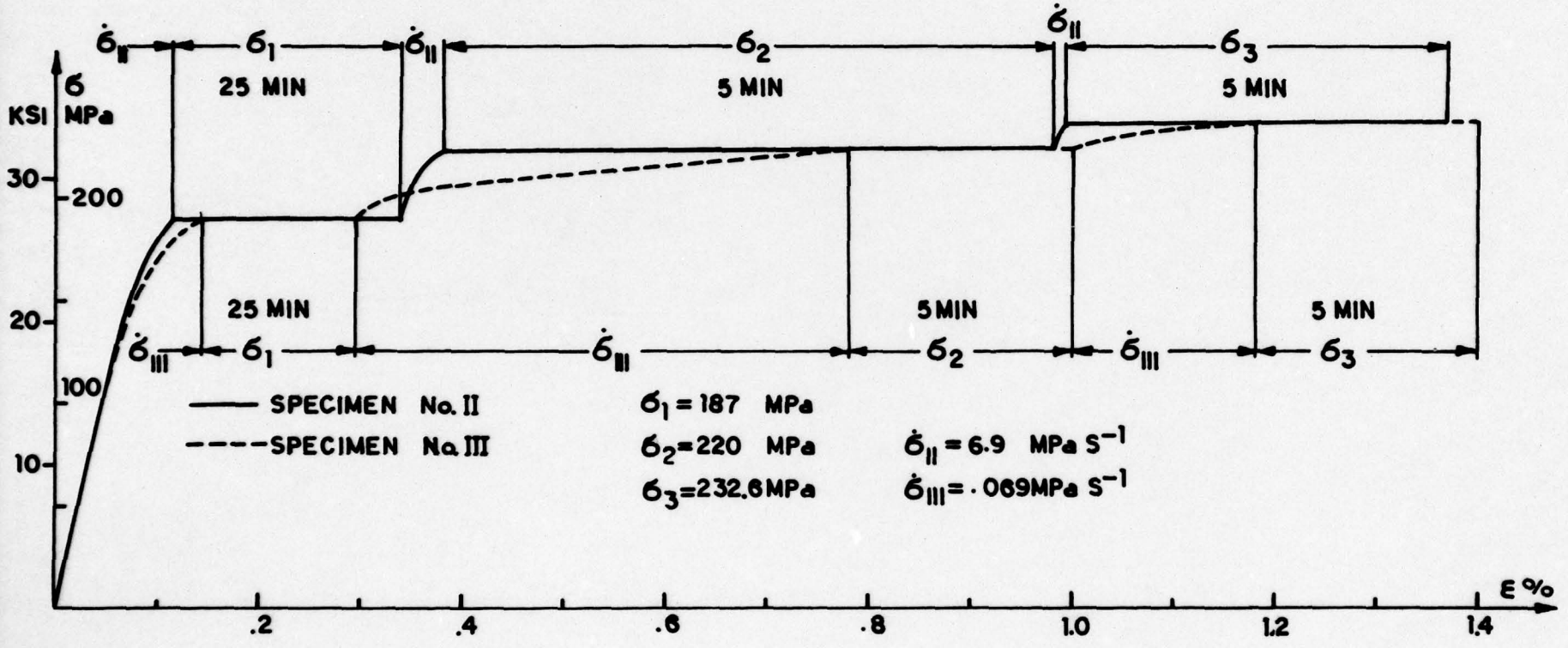
σ̇II
σ1
25 MIN
σ̇II
σ2
5 MIN
σ̇II
σ3
5 MIN
σ
KSI
MPa
30
200
20
25 MIN
5 MIN
5 MIN
σ̇III
σ1
σ̇II
σ2
σ̇III
σ3
100
10
SPECIMEN No. II
SPECIMEN No. III
σ1 = 187 MPa
σ2 = 220 MPa
σ3 = 232.6 MPa
σ̇II = 6.9 MPa S−1
σ̇III = .069 MPa S−1
ε %
.2
.4
.6
.8
1.0
1.2
1.4

Figure 2

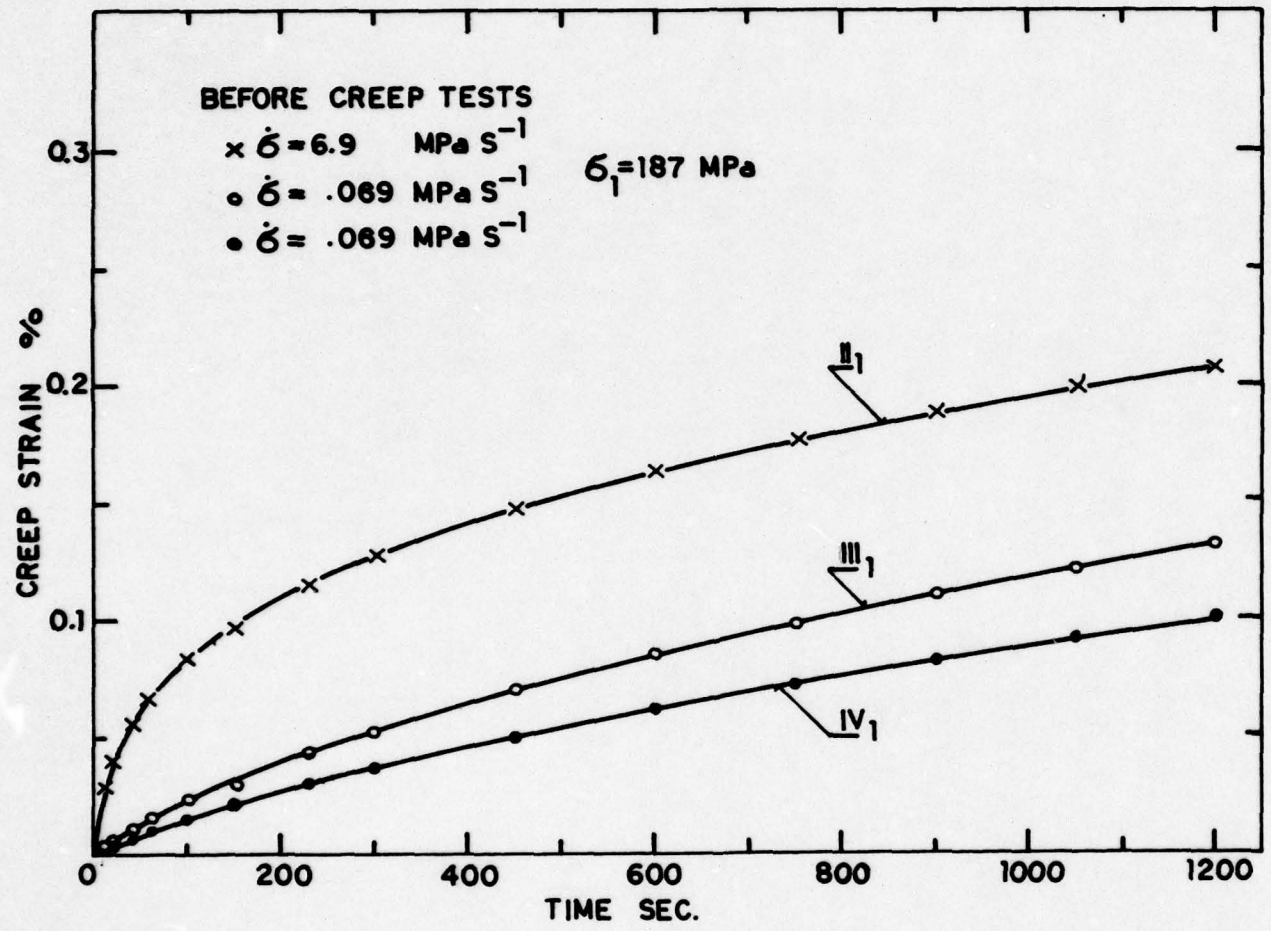
BEFORE CREEP TESTS
× σ̇ = 6.9 MPa S⁻¹
∘ σ̇ = .069 MPa S⁻¹
• σ̇ = .069 MPa S⁻¹
σ1 = 187 MPa
II1
III1
IV1
CREEP STRAIN %
0.3
0.2
0.1
0
200
400
600
800
1000
1200
TIME SEC.

Figure 3

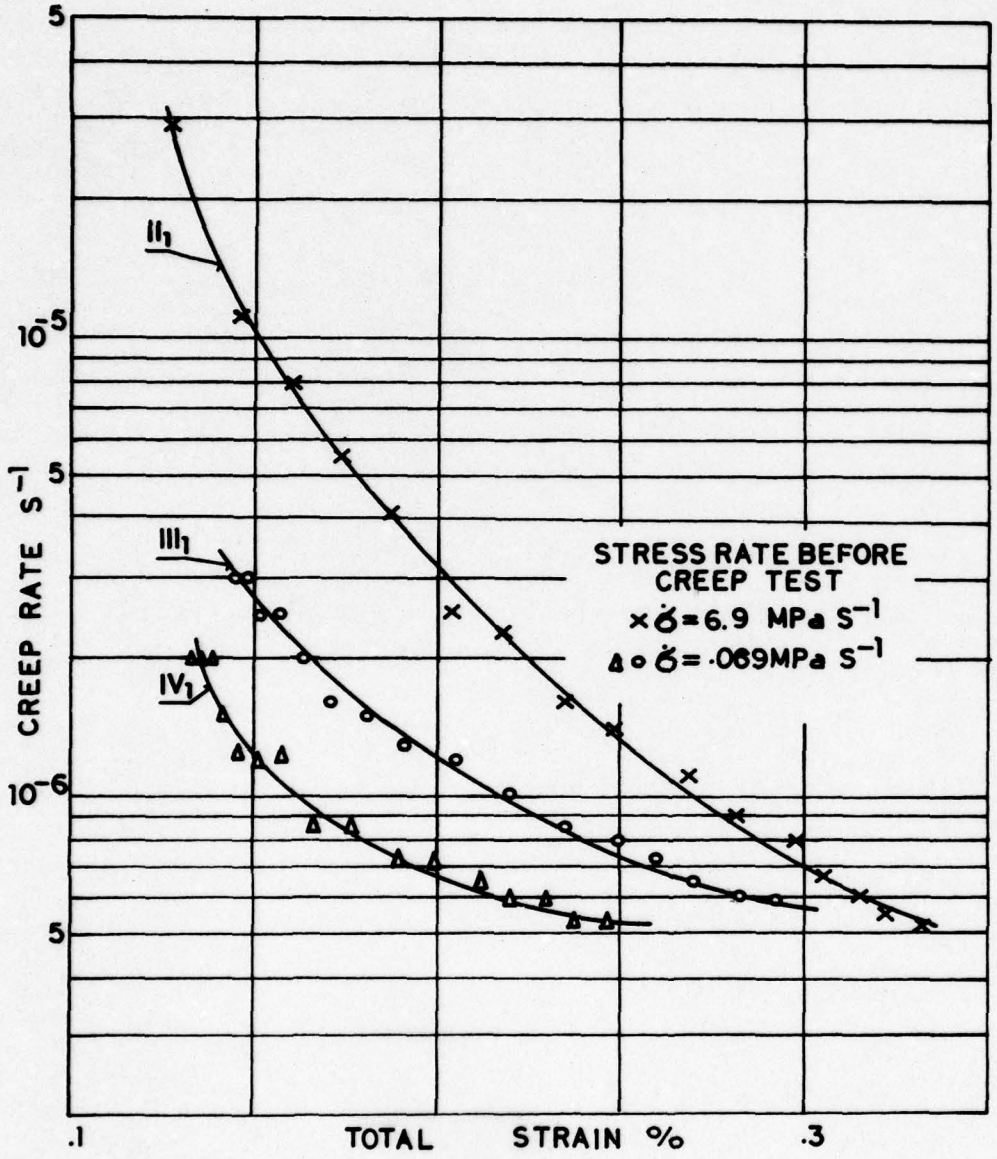
5
10^{-5}
5
10^{-6}
5
CREEP RATE S^{-1}
II1
III1
IV1
STRESS RATE BEFORE CREEP TEST
× $\dot{\sigma}$ = 6.9 MPa S^{-1}
Δ ○ $\dot{\sigma}$ = .069MPa S^{-1}
.1
TOTAL STRAIN %
.3

Figure 4

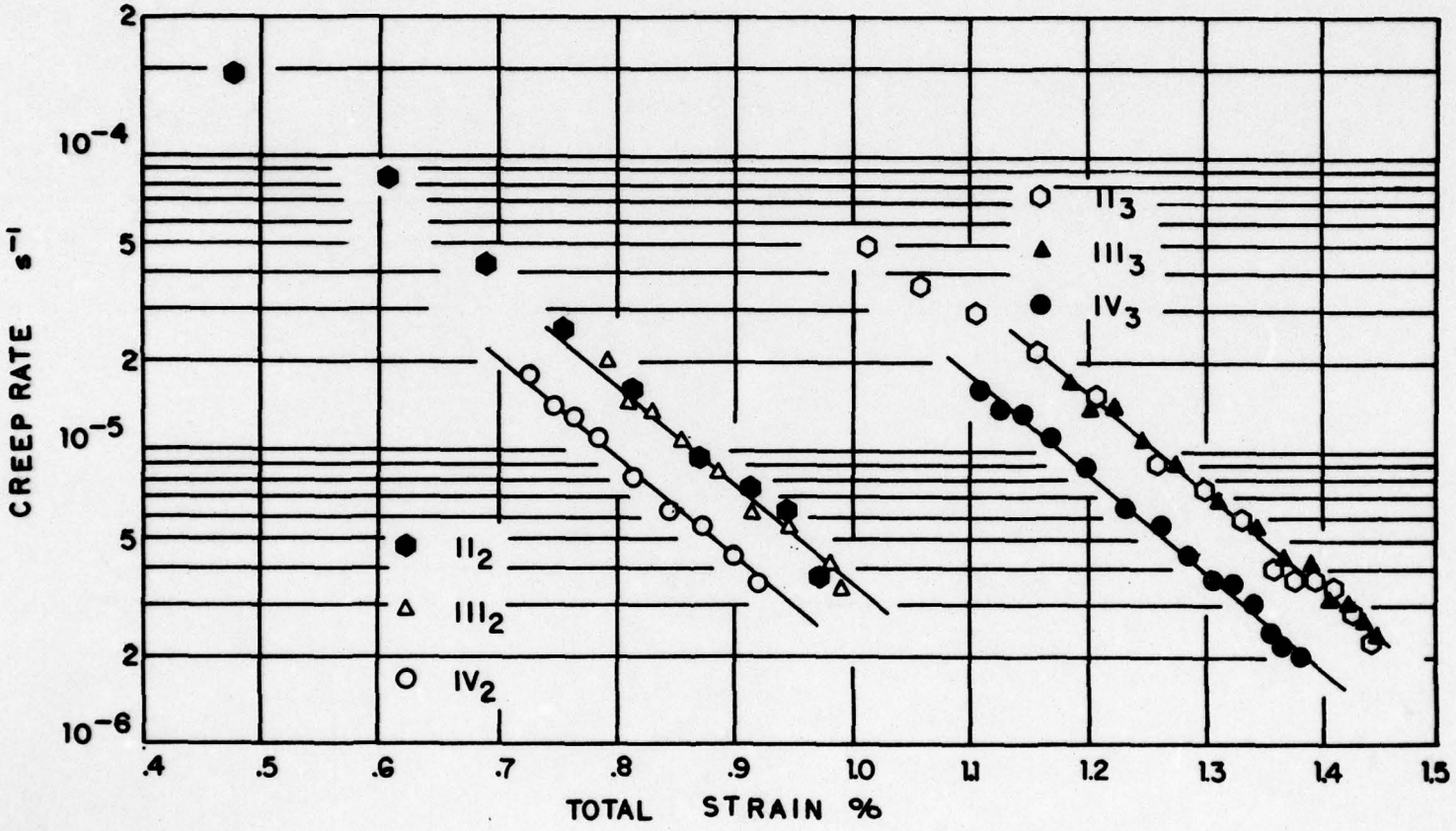
CREEP RATE s⁻¹
2
10⁻⁴
5
2
10⁻⁵
5
2
10⁻⁶
.4
.5
.6
.7
.8
.9
1.0
1.1
1.2
1.3
1.4
1.5
TOTAL STRAIN %
II2
III2
IV2
II3
III3
IV3

Figure 5

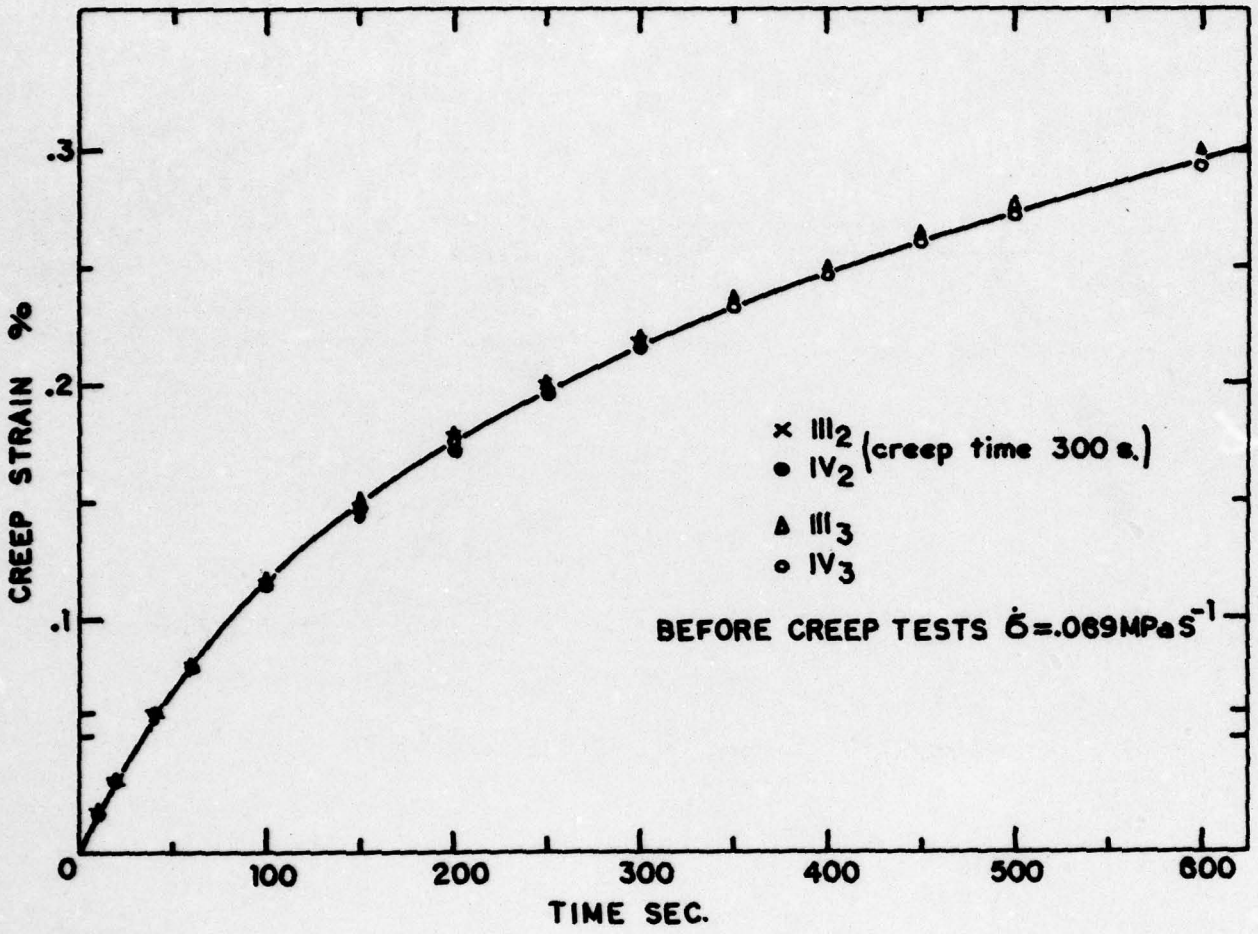
CREEP STRAIN %
.3
.2
.1
0
100
200
300
400
500
600
TIME SEC.
× III2
• IV2 (creep time 300 s.)
▲ III3
○ IV3
BEFORE CREEP TESTS σ̇=.069MPa·S⁻¹

Figure 6

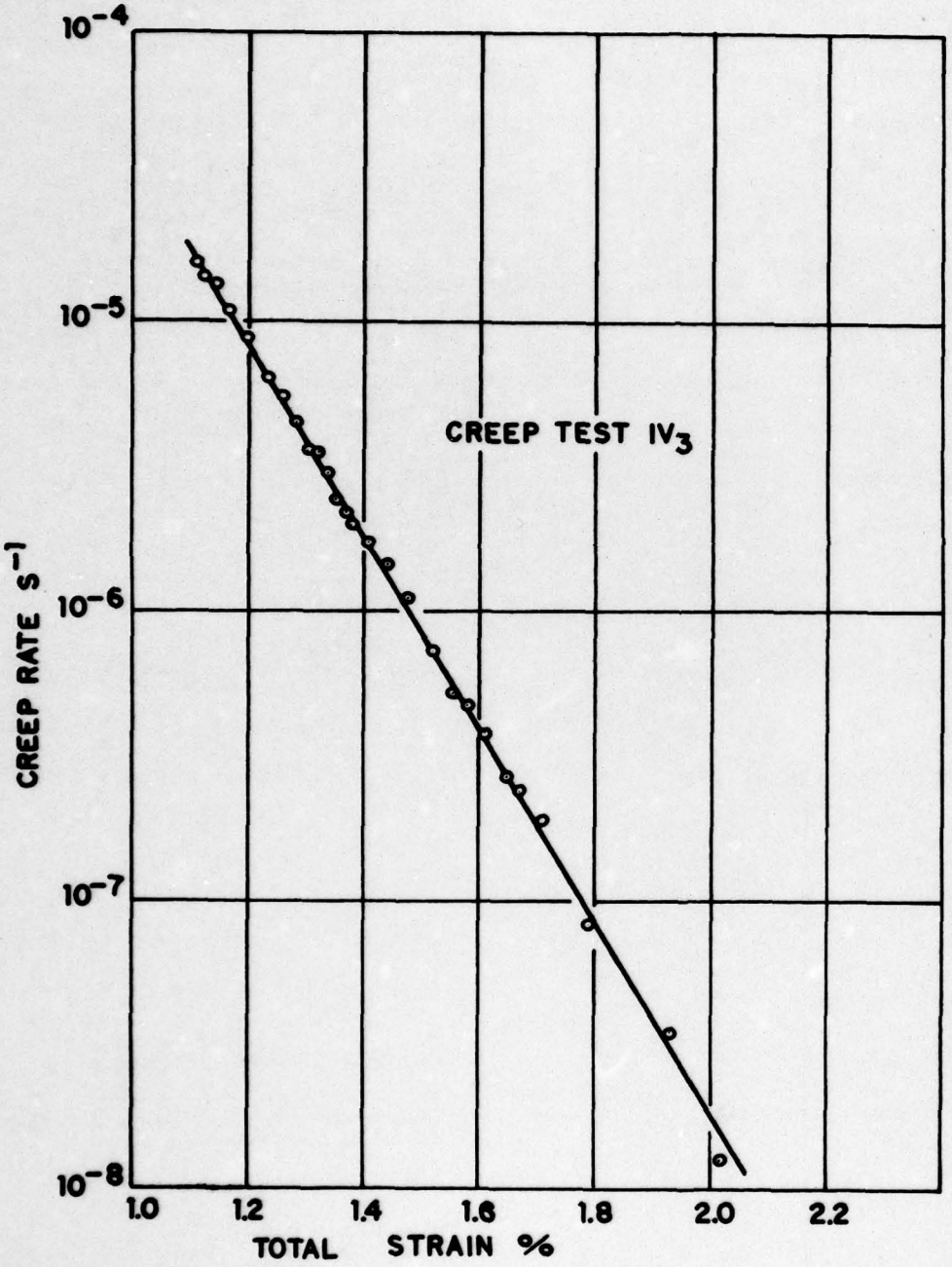
10^{-4}
10^{-5}
10^{-6}
10^{-7}
10^{-8}
CREEP RATE S^{-1}
CREEP TEST IV_3
1.0
1.2
1.4
1.6
1.8
2.0
2.2
TOTAL STRAIN %

Figure 7

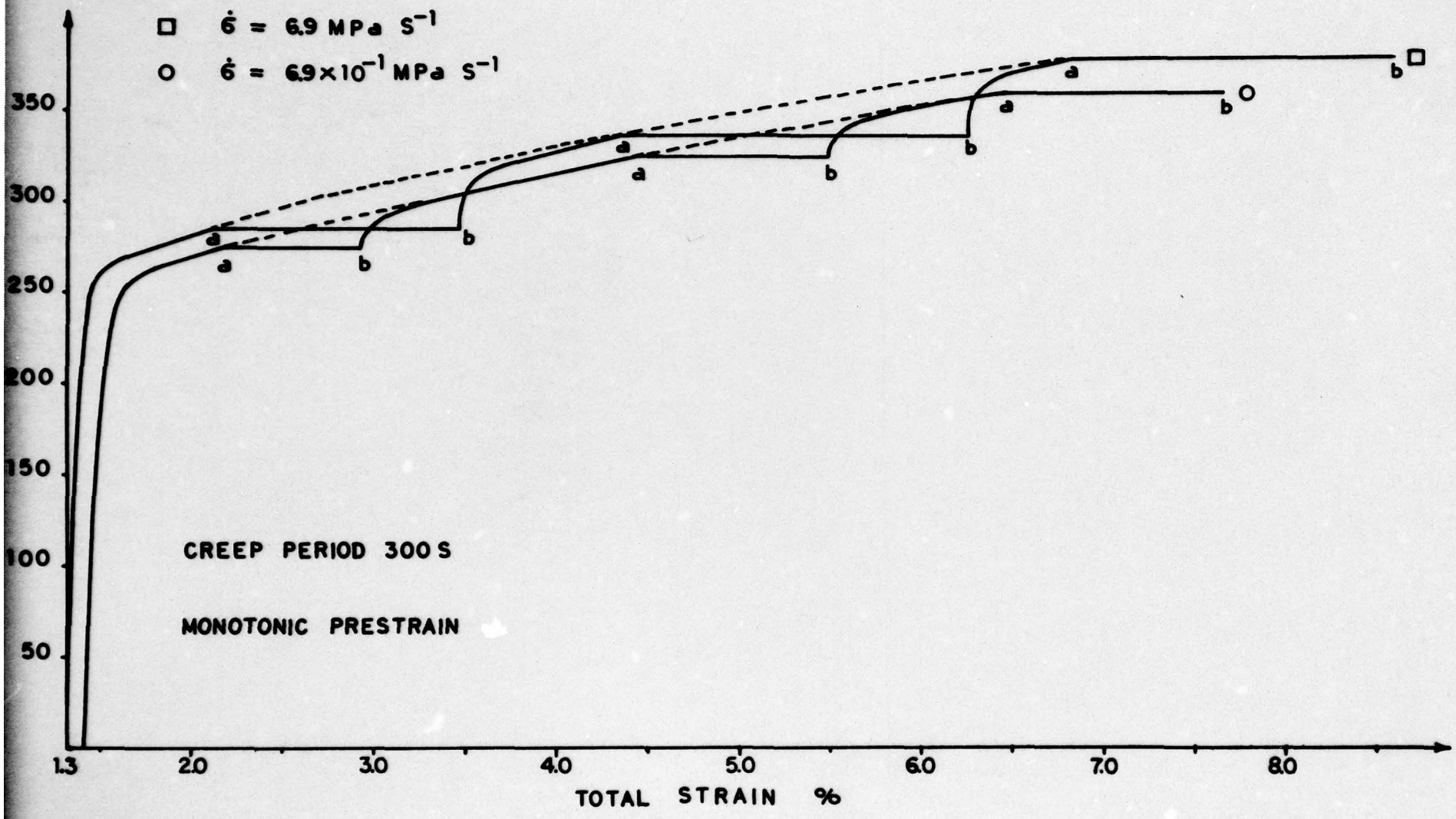
□ $\dot{\epsilon}$ = 6.9 MPa S^{-1}
○ $\dot{\epsilon}$ = 6.9×10^{-1} MPa S^{-1}
350
300
250
200
150
100
50
CREEP PERIOD 300 S
MONOTONIC PRESTRAIN
1.3
2.0
3.0
4.0
5.0
6.0
7.0
8.0
TOTAL STRAIN %
a
b

Figure 8

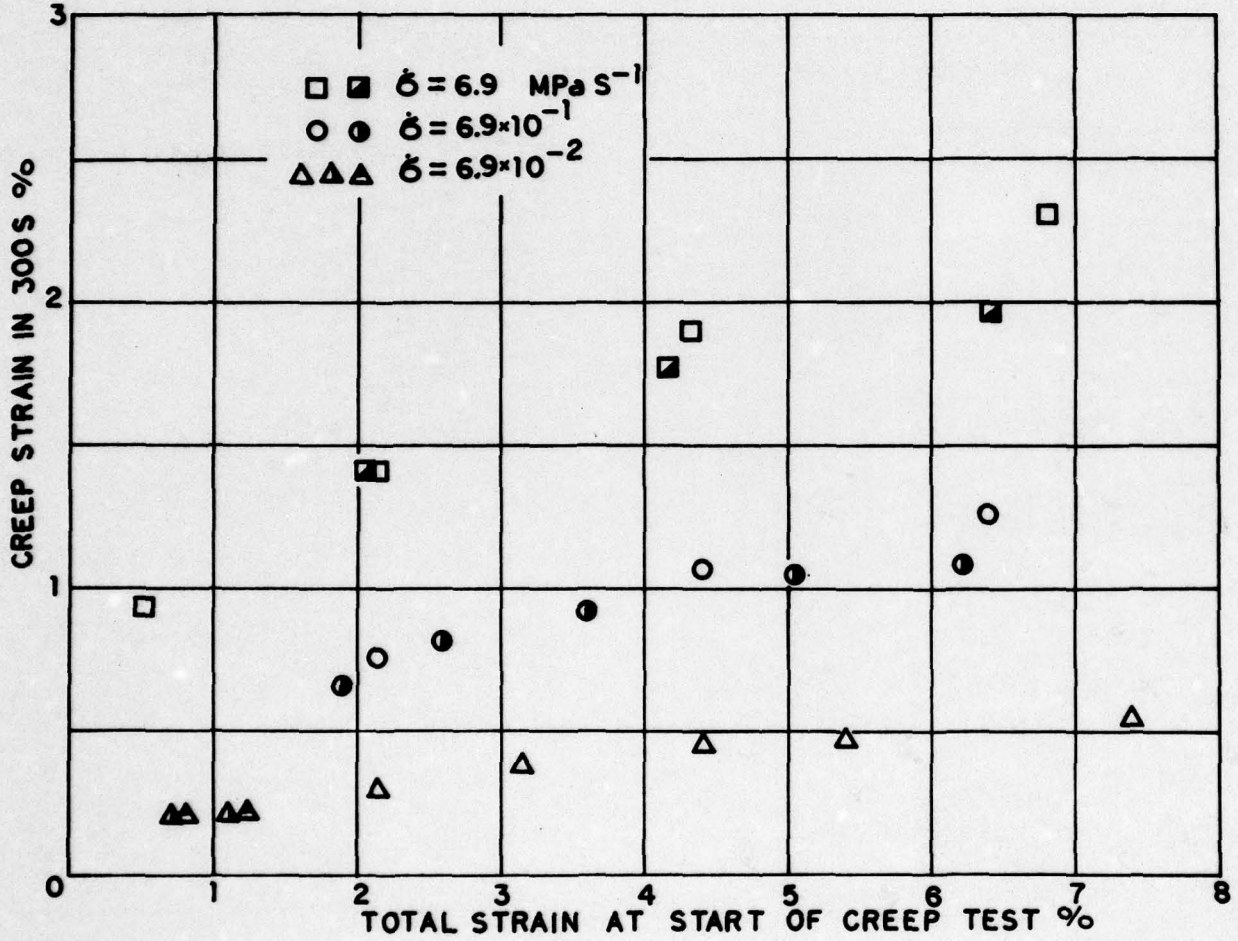
□ ■ $\dot{\sigma} = 6.9$ MPa S^{-1}
○ ● $\dot{\sigma} = 6.9 \times 10^{-1}$
△△△ $\dot{\sigma} = 6.9 \times 10^{-2}$
CREEP STRAIN IN 300S %
TOTAL STRAIN AT START OF CREEP TEST %
0
1
2
3
4
5
6
7
8

Figure 9

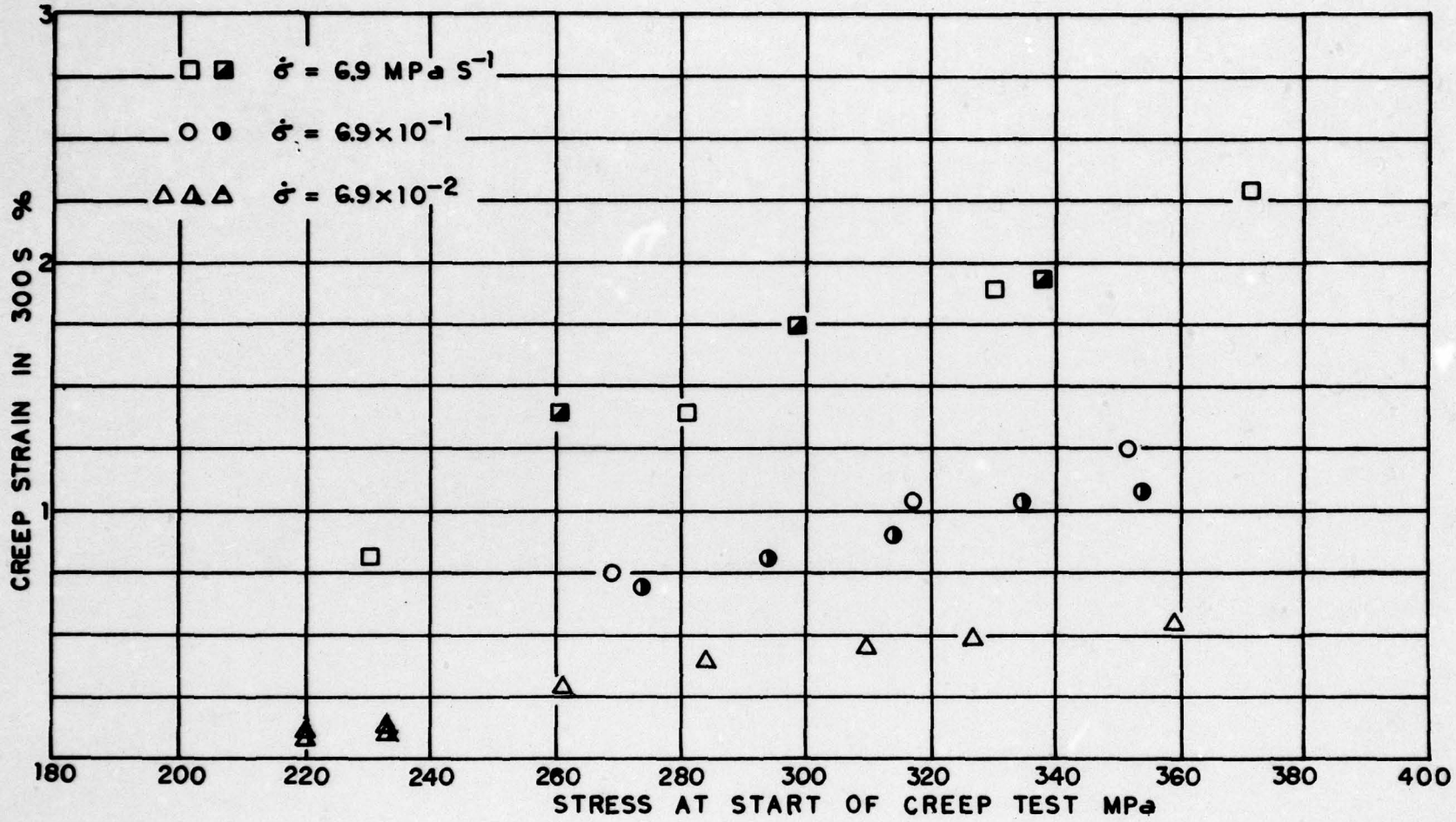
□ ■ $\dot{\sigma}$ = 6.9 MPa S^{-1}
○ ◐ $\dot{\sigma}$ = 6.9×10^{-1}
△△△ $\dot{\sigma}$ = 6.9×10^{-2}
CREEP STRAIN IN 300 S %
3
2
1
180
200
220
240
260
280
300
320
340
360
380
400
STRESS AT START OF CREEP TEST MPa

Figure 10

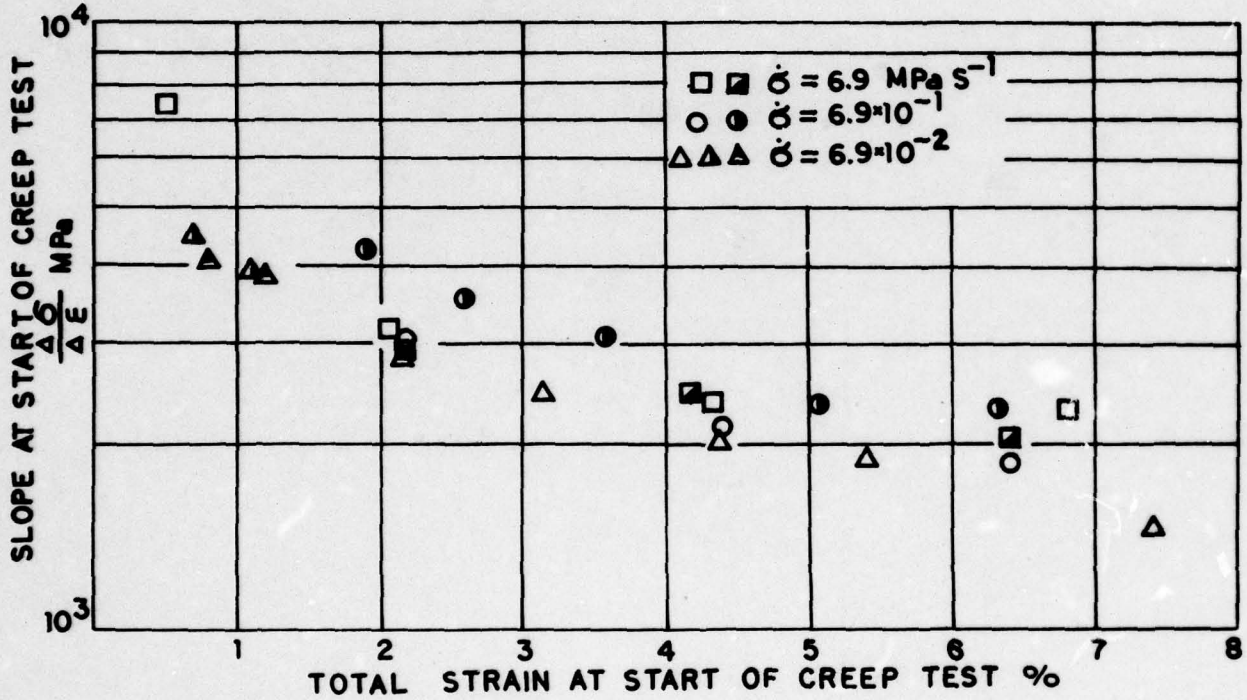
10^4
10^3
SLOPE AT START OF CREEP TEST $\frac{\Delta\sigma}{\Delta\varepsilon}$ MPa
$\dot{\sigma} = 6.9$ MPa S^{-1}
$\dot{\sigma} = 6.9\times10^{-1}$
$\dot{\sigma} = 6.9\times10^{-2}$
1
2
3
4
5
6
7
8
TOTAL STRAIN AT START OF CREEP TEST %

Figure 11

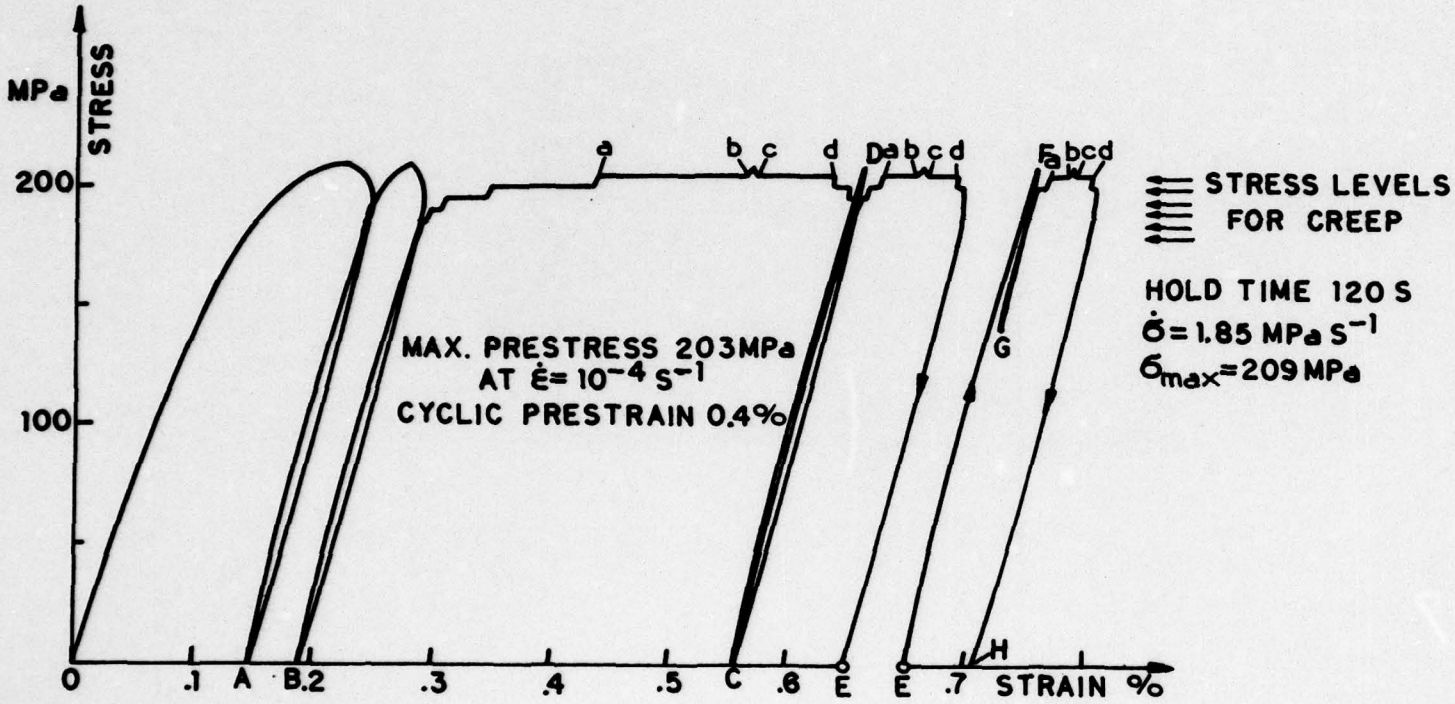
MPa
STRESS
200
100
0
.1
A
B.2
.3
.4
.5
C
.6
E
E
.7
STRAIN %
a
b
c
d
D
a
b
c
d
F
a
b
c
d
G
H
MAX. PRESTRESS 203MPa
AT $\dot{\varepsilon} = 10^{-4}\ s^{-1}$
CYCLIC PRESTRAIN 0.4%
STRESS LEVELS
FOR CREEP
HOLD TIME 120 S
$\dot{\sigma} = 1.85\ MPa\ s^{-1}$
$\sigma_{max} = 209\ MPa$

Figure 12

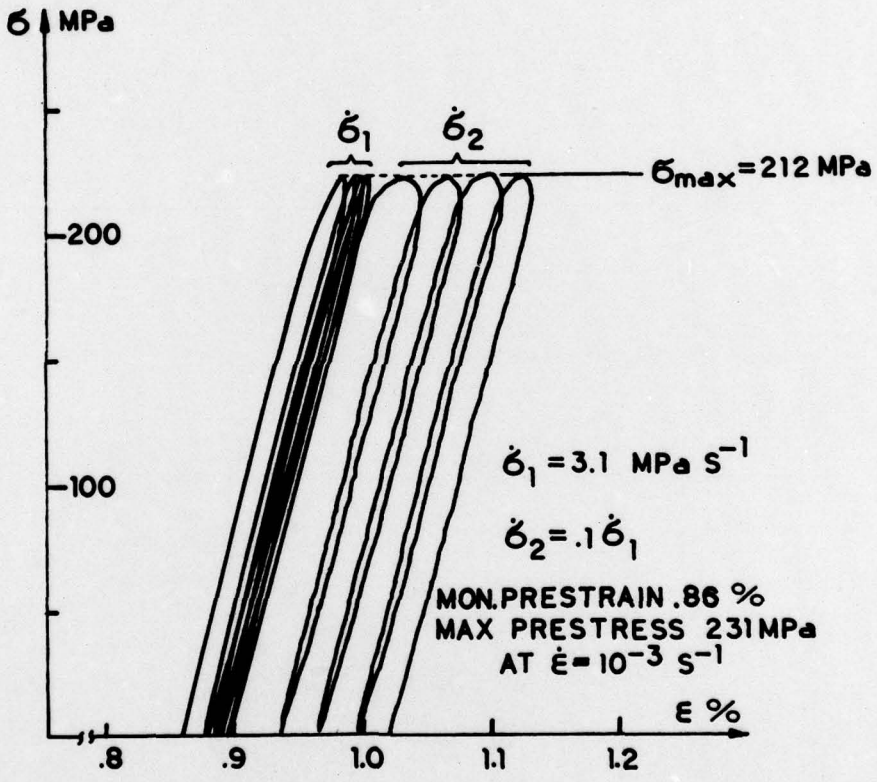
σ MPa
200
100
σ̇1
σ̇2
σmax=212 MPa
σ̇1 = 3.1 MPa s-1
σ̇2 = .1 σ̇1
MON. PRESTRAIN .86 %
MAX PRESTRESS 231 MPa
AT ε̇ = 10-3 s-1
ε %
.8
.9
1.0
1.1
1.2

Figure 13

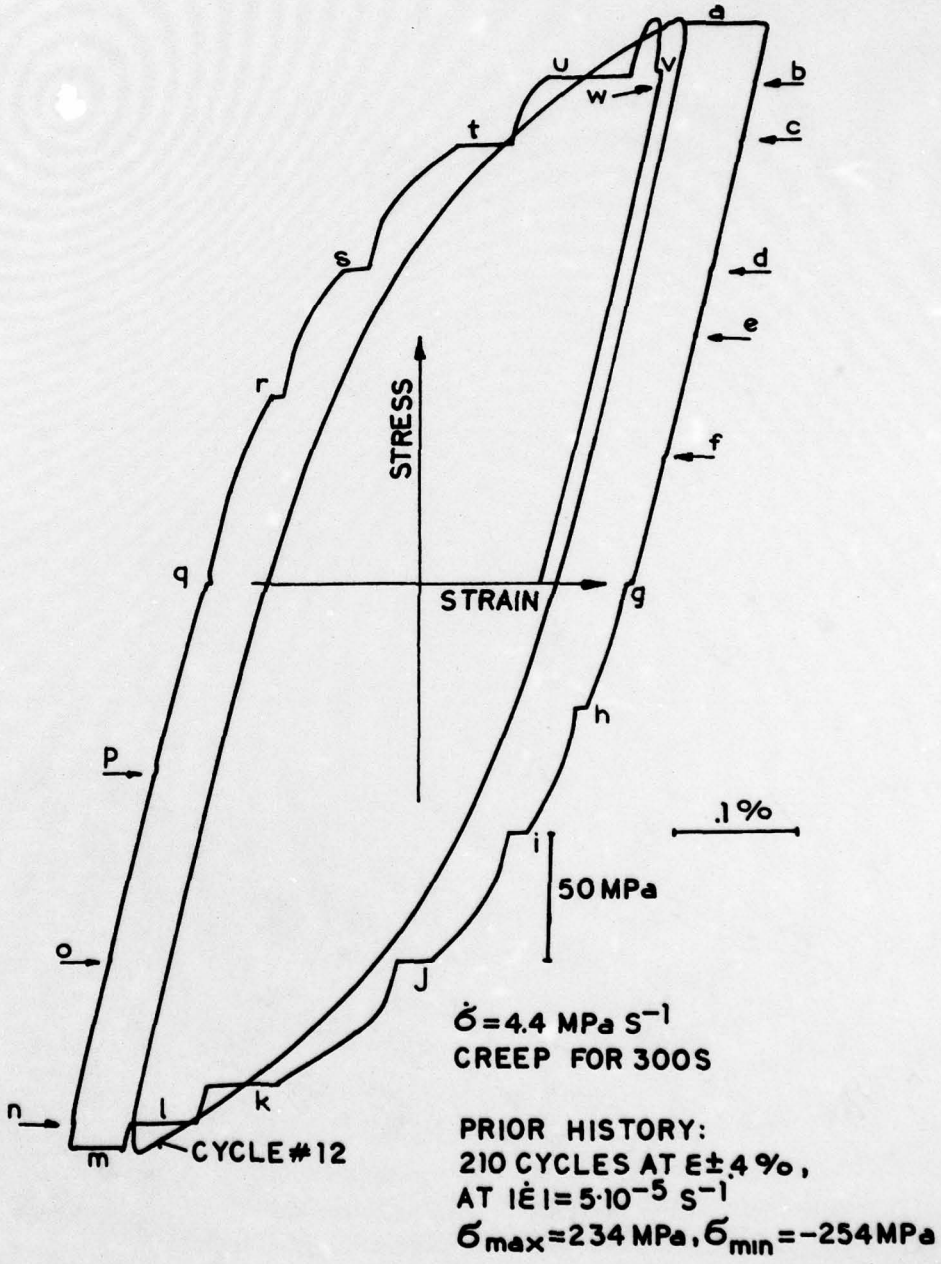
a
b
c
d
e
f
g
h
i
J
k
l
m
n
o
p
q
r
s
t
u
v
w
STRESS
STRAIN
.1%
50 MPa
σ̇ = 4.4 MPa S⁻¹
CREEP FOR 300S
PRIOR HISTORY:
210 CYCLES AT E±.4%,
AT |Ė| = 5·10⁻⁵ S⁻¹
σmax = 234 MPa, σmin = −254 MPa
CYCLE #12

Figure 14a

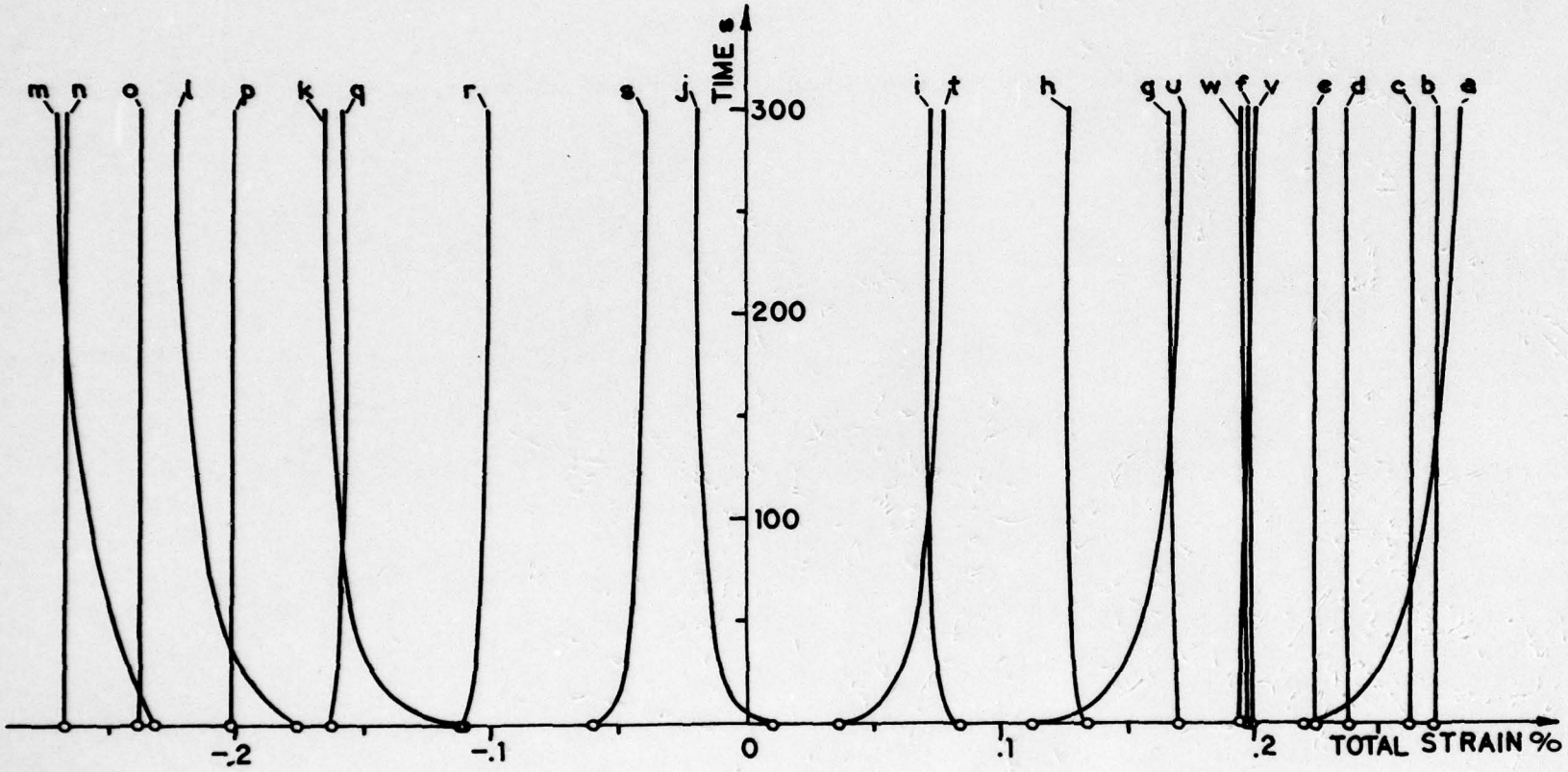
TIME s
300
200
100
m
n
o
l
p
k
q
r
s
j
i
t
h
g
u
w
f
v
e
d
c
b
a
-.2
-.1
0
.1
.2
TOTAL STRAIN %

Figure 14b

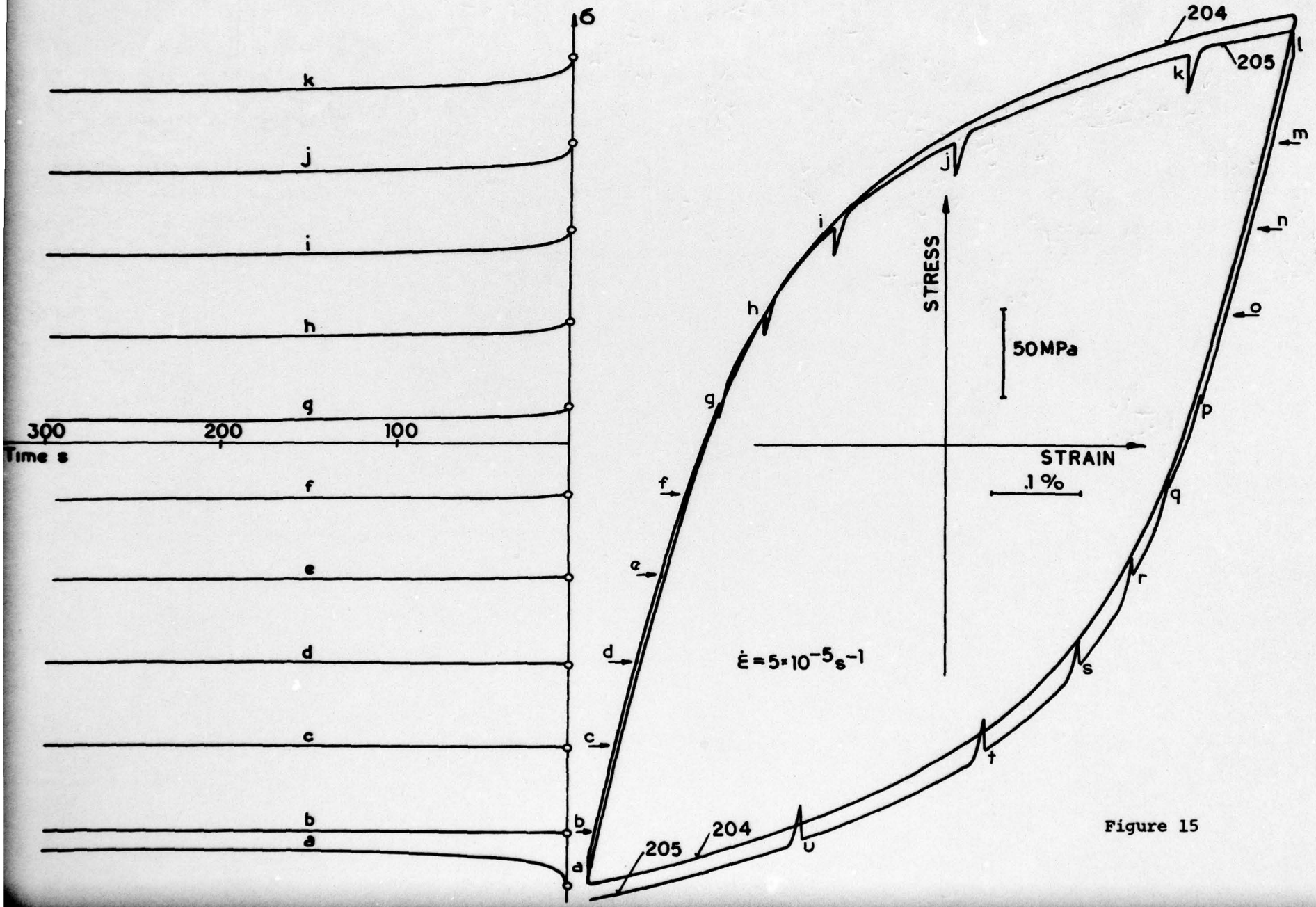
σ
k
j
i
h
g
300
200
100
Time s
f
e
d
c
b
a
STRESS
50MPa
STRAIN
.1 %
$\dot{E}=5\cdot10^{-5}s^{-1}$
204
205
l
m
n
o
p
q
r
s
t
u

Figure 15

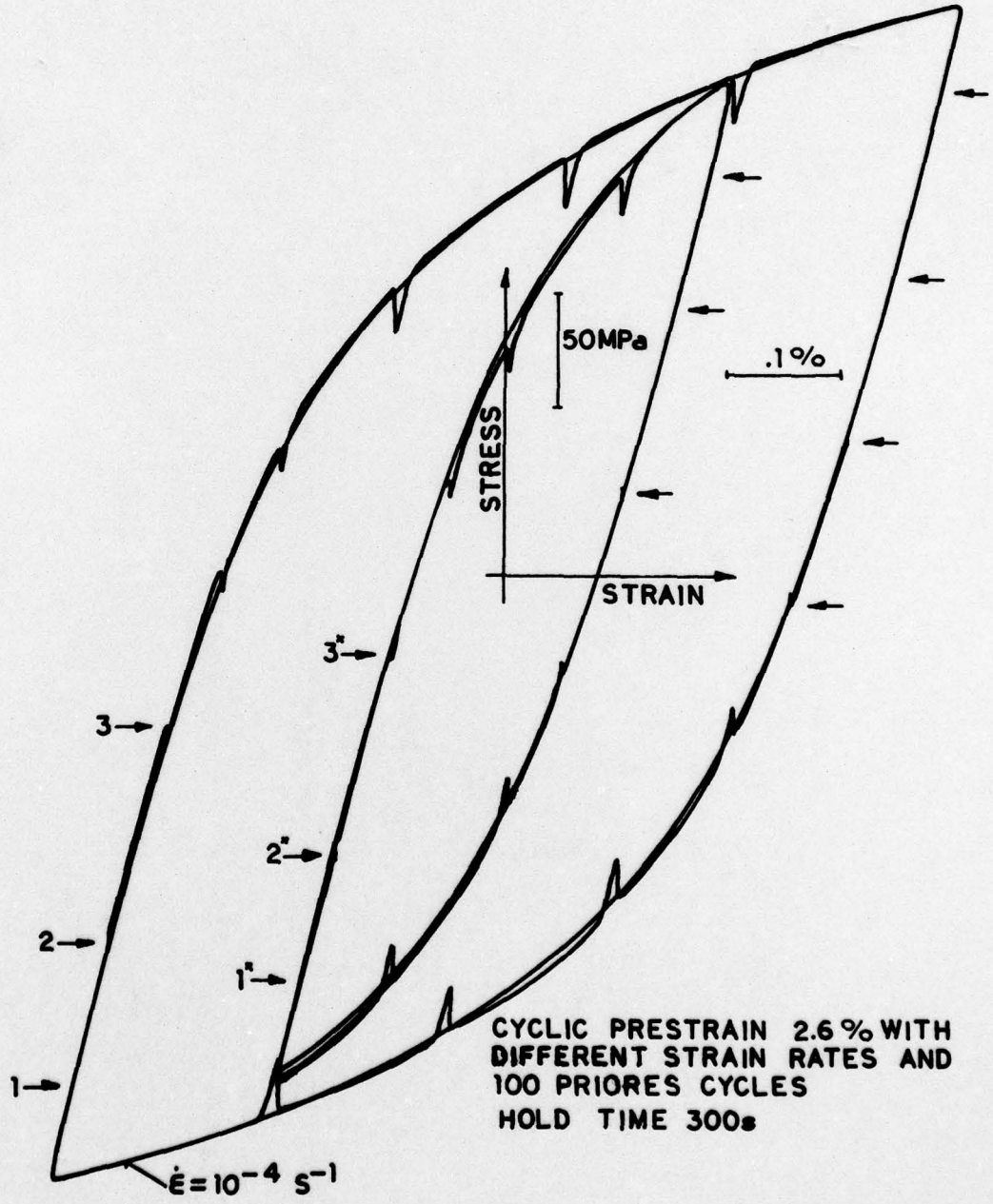
50MPa
.1%
STRESS
STRAIN
3*
3
2*
2
1*
1
CYCLIC PRESTRAIN 2.6% WITH
DIFFERENT STRAIN RATES AND
100 PRIORES CYCLES
HOLD TIME 300s
$\dot{\varepsilon} = 10^{-4}\ s^{-1}$

Figure 16

Unclassified

SECURITY CLASSIFICATION OF THIS PAGE (When Data Entered)

REPORT DOCUMENTATION PAGE

READ INSTRUCTIONS BEFORE COMPLETING FORM

1. REPORT NUMBER: RPI-CS-79-4
2. GOVT ACCESSION NO.
3. RECIPIENT'S CATALOG NUMBER

4. TITLE (and Subtitle): Uniaxial Creep, Cyclic Creep and Relaxation of AISI Type 304 Stainless Steel at Room Temperature. An Experimental Study.
5. TYPE OF REPORT & PERIOD COVERED: Topical Report
6. PERFORMING ORG. REPORT NUMBER: RPI CS 79-4

7. AUTHOR(s): D. Kujawski, V. Kallianpur and E. Krempl
8. CONTRACT OR GRANT NUMBER(s): N0014-76-C-0231

9. PERFORMING ORGANIZATION NAME AND ADDRESS: Department of Mechanical Engineering, Aeronautical Engineering & Mechanics, Rensselaer Polytechnic Institute, Troy, NY 12181
10. PROGRAM ELEMENT, PROJECT, TASK AREA & WORK UNIT NUMBERS: NR 064-571

11. CONTROLLING OFFICE NAME AND ADDRESS: Dept. of the Navy, Office of Naval Research, Structural Mechanics Program, Arlington, VA 22217
12. REPORT DATE: August 1979
13. NUMBER OF PAGES: 42

14. MONITORING AGENCY NAME & ADDRESS (if different from Controlling Office): Office of Naval Research - Resident Representative, 715 Broadway - Fifth Floor, New York, NY 10003
15. SECURITY CLASS. (of this report): Unclassified
15a. DECLASSIFICATION/DOWNGRADING SCHEDULE

16. DISTRIBUTION STATEMENT (of this Report)

Approved for public release; distribution unlimited.

17. DISTRIBUTION STATEMENT (of the abstract entered in Block 20, if different from Report)

18. SUPPLEMENTARY NOTES

19. KEY WORDS (Continue on reverse side if necessary and identify by block number)

Creep, relaxation, plastic flow, 304 stainless steel, room temperature, cyclic creep, ratchetting, viscoplasticity, inelastic behavior.

20. ABSTRACT (Continue on reverse side if necessary and identify by block number)

A servocontrolled testing machine and strain measurement at the gage length were used to study the uniaxial rate(time)-dependent behavior of AISI Type 304 Stainless Steel at room temperature. The creep strain accumulated in a given period of time depends strongly on the stress rate preceding the creep test. In constant stress rate zero-to-tension loading the creep strain accumulated in a fixed time period at a given stress level is always higher during loading than during unloading. Continued cycling causes an exhaustion of creep

DD FORM 1 JAN 73 1473 EDITION OF 1 NOV 65 IS OBSOLETE
S/N 0102-LF-014-6601

Unclassified

SECURITY CLASSIFICATION OF THIS PAGE (When Data Entered)

ratchetting which depends on the stress rate. Periods of creep and relaxation introduced during completely reversed plastic cycling show that the curved portions of the hysteretic loop exhibit most of the inelasticity. In the straight portions creep and relaxation are small and there exists a region commencing after unloading where the behavior is similar to that at the origin for virgin materials. This region does not extend to zero stress.

The results are at variance with creep theory and with viscoplasticity theories which assume that the yield surface expands with the stress. They support the theory of viscoplasticity based on total strain and overstress.